2022.07.19 SPICE workshop

# Observation of the orbital Hall effect in a light metal Ti

http://arxiv.org/abs/2109.14847

Young-Gwan Choi†, Daegeun Jo†, Kyung-Hun Ko†, Dongwook Go, Kyung-Han Kim, Hee Gyum Park, Changyoung Kim, Byoung-Chul Min, **Gyung-Min Choi**★, and Hyun-Woo Lee★

Department of Energy Science, Sungkyunkwan University

Center for Integrated Nanostructured Physics, Institute of Basic Science

# Acknowledgment

## Measurement

**Young-Gwan Choi, Kyung-Hun Ko**, Gyung-Min Choi at SKKU

## Theory

**Daegeun Jo**, Dongwook Go, Kyung-Han Kim, Hyun-Woo Lee at Postech

## Sample fabrication

Kyung-Hun Ko, Young-Gwan Choi, Gyung-Min Choi at SKKU

Hee Gyum Park, Byoung-Chul Min at KIST

## Initial idea

Changyoung Kim at SNU

## Funding

National Research Foundation of Korea

# Outline

1. **Introduction**

   Orbital Hall effect vs Spin Hall effect

   Experimental method: Magneto-optical Kerr effect

2. **Results and discussion Orbital accumulation**

   Orbital accumulation on Ti surface

   Orbital torque in Ti/FM structure

3. **Summary**

# Orbital Hall effect and spin Hall effect

## Spin Hall effect

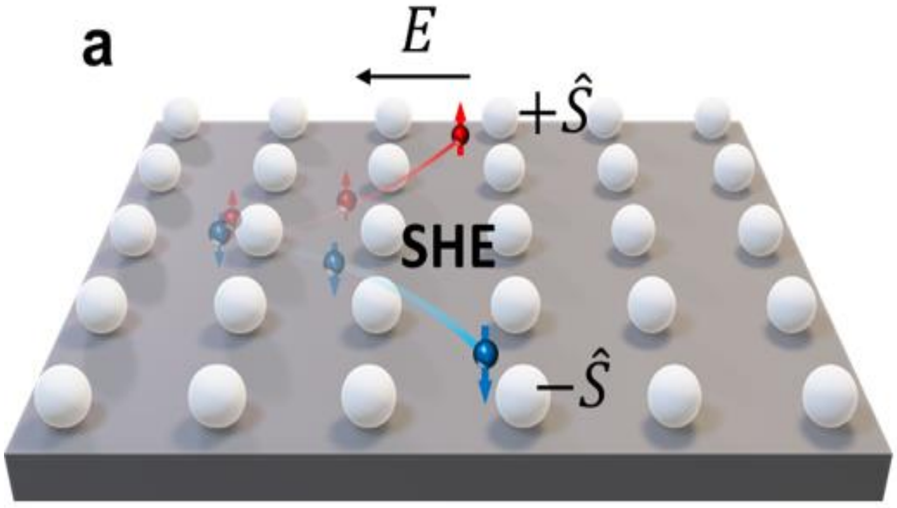

## Orbital Hall effect

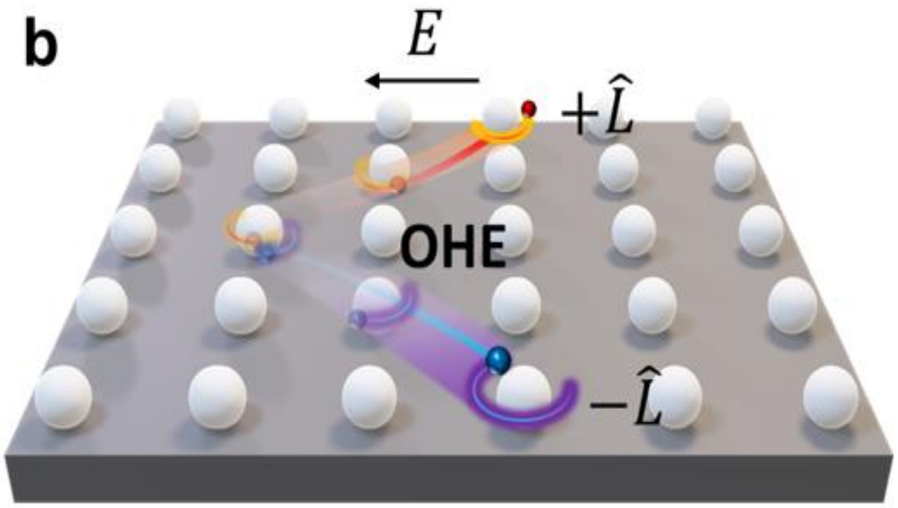

Spin Hall effect: exist at heavy metals, which has a strong spin-orbit coupling (SOC).

Orbital Hall effect: exist at wide range materials, even without SOC.

# Orbital Hall effect from orbital texture

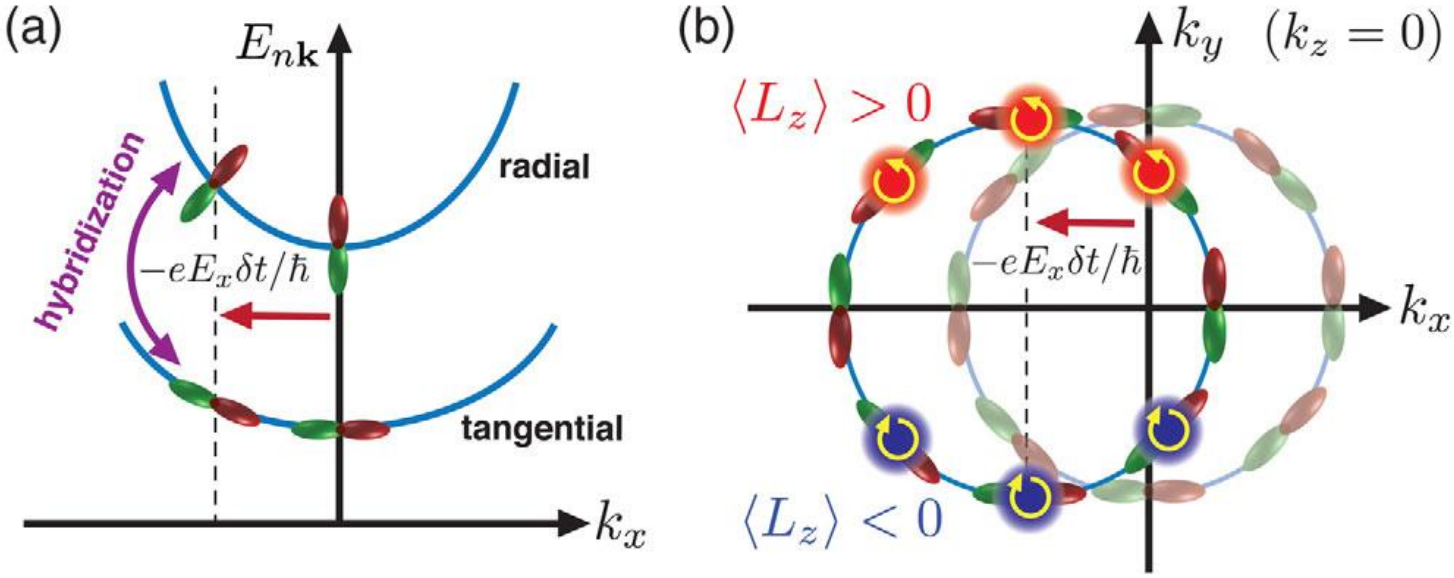

Go et al., PRL, 121, 086602 (2018)

The orbital character varies with k and from bands to bands.

E-field → k-vector shift → interband superposition → $\left|p_x\right\rangle \pm i\left|p_y\right\rangle = |L_z = \pm\hbar\rangle$

Dynamically induced interband superposition can lead to non-zero orbital (*L*).

# Orbital Hall conductivity of Ti

Electronic band structure

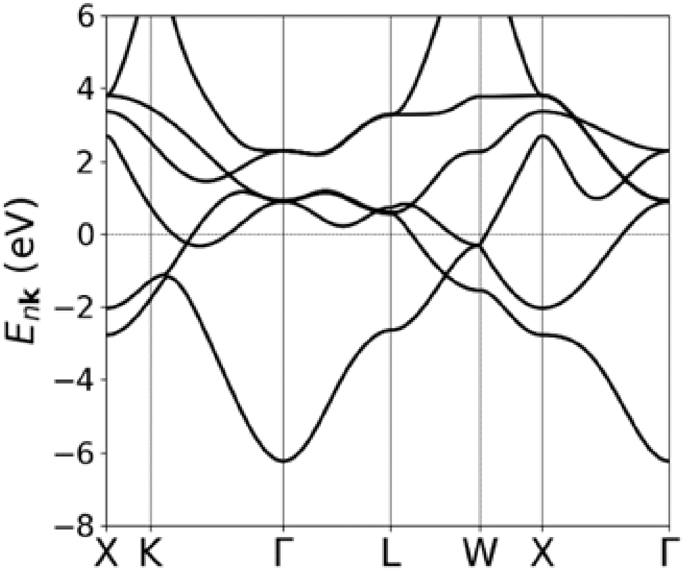

Orbital texture

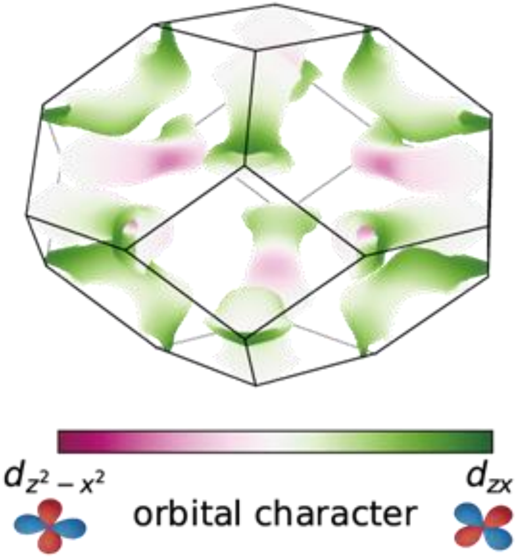

Orbital Hall conductivity

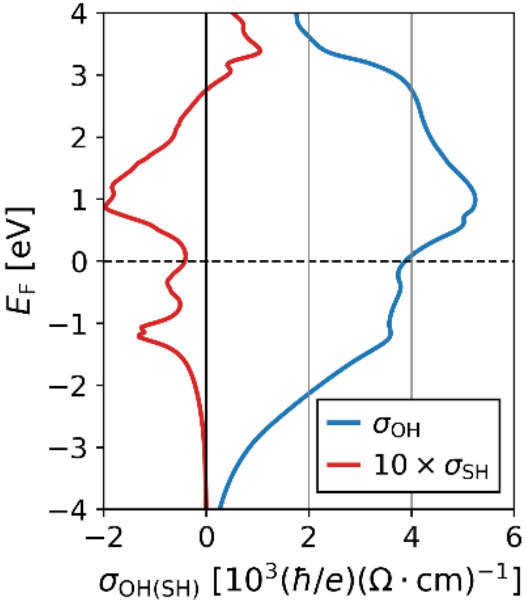

$$\sigma_{OH(SH)} = \frac{ie\hbar}{N_{\mathbf{k}}V_{cell}}\sum_{\mathbf{k}}\sum_{n\neq m}(f_{n\mathbf{k}}-f_{m\mathbf{k}})\frac{\langle u_{n\mathbf{k}}|j_z^{L_y(S_y)}|u_{m\mathbf{k}}\rangle\langle u_{m\mathbf{k}}|v_x|u_{n\mathbf{k}}\rangle}{(E_{n\mathbf{k}}-E_{m\mathbf{k}}+i\Gamma)^2}$$

$\sigma_{\mathrm{OH}}, 3800\ \left(\frac{\hbar}{e}\right)(\Omega\cdot\mathrm{cm})^{-1}$, is ~100 times larger than $\sigma_{\mathrm{SH}}, -40\ \left(\frac{\hbar}{e}\right)(\Omega\cdot\mathrm{cm})^{-1}$.

# Experimental methods

## Optical detection: Magneto-optical Kerr effect (MOKE)

Sensitive detection: light is much more sensitive on orbital than spin.
Vector detection: light can distinguish $M_y$ and $M_z$ components.

Orbital accumulation

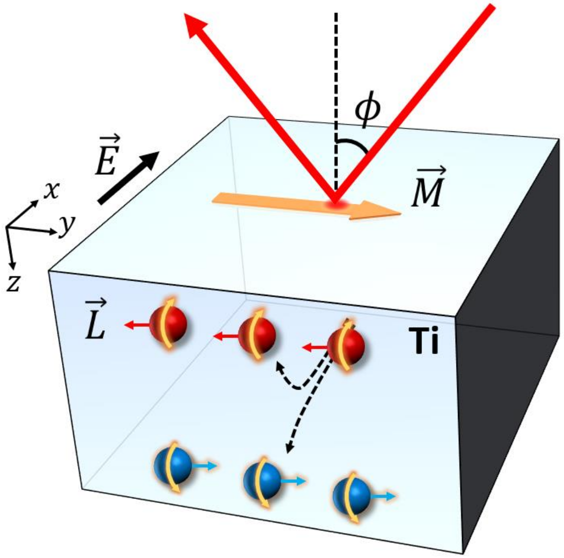

Orbital torque

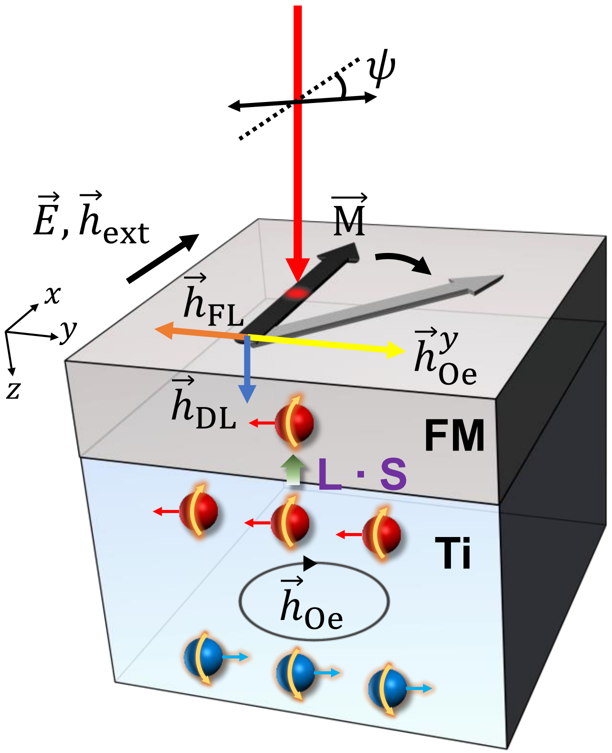

# MOKE from spin Hall effect

Polar MOKE

GaAs

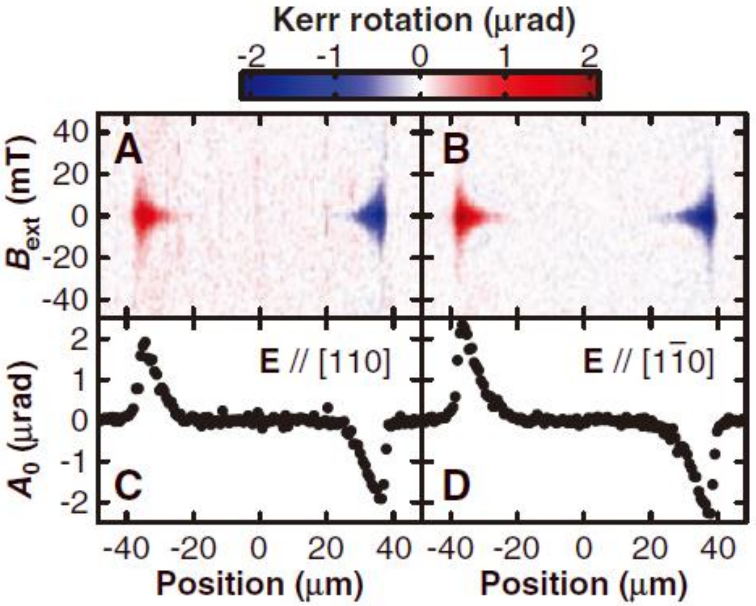

Kato et al., Science, 306, 1910 (2004)

Longitudinal MOKE

Pt

W

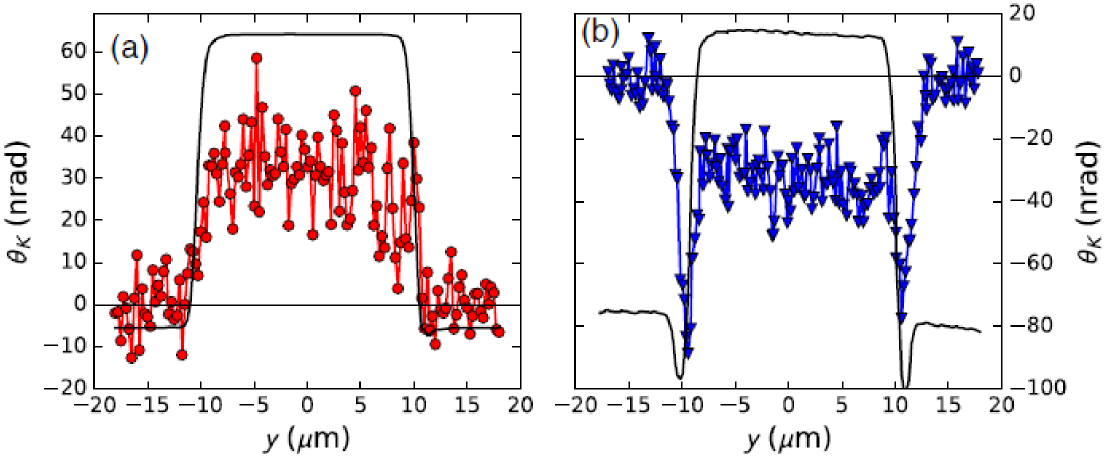

Stamm et al., PRL, 119, 087203 (2017)

Magneto-optical Kerr effect (MOKE) has been used to detect SHE-induced spin accumulation on edge or surface of semiconductors and metals.

# Experimental setup

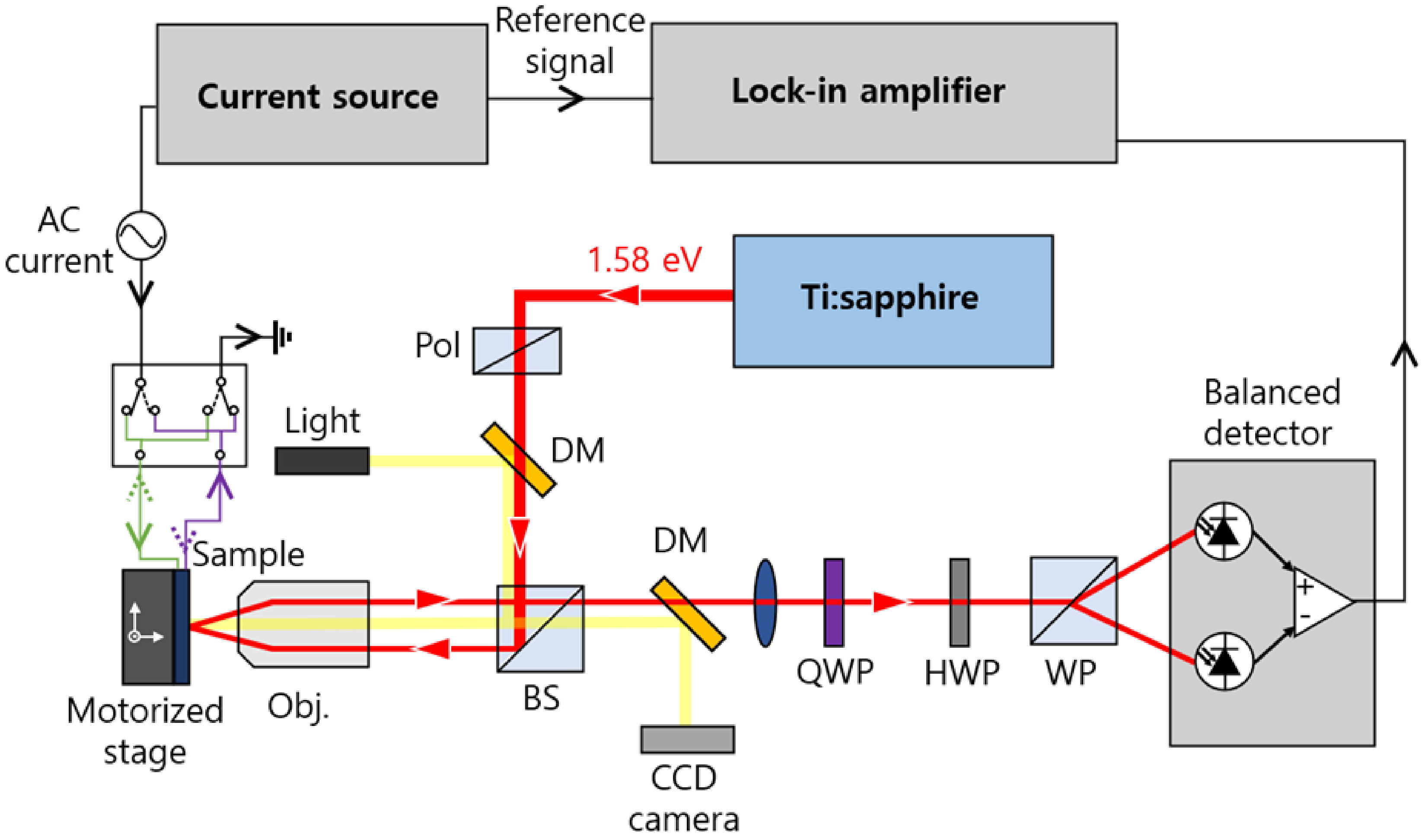

Kerr rotation resolution: <10 nrad

# Part 1: orbital accumulation

Orbital accumulation

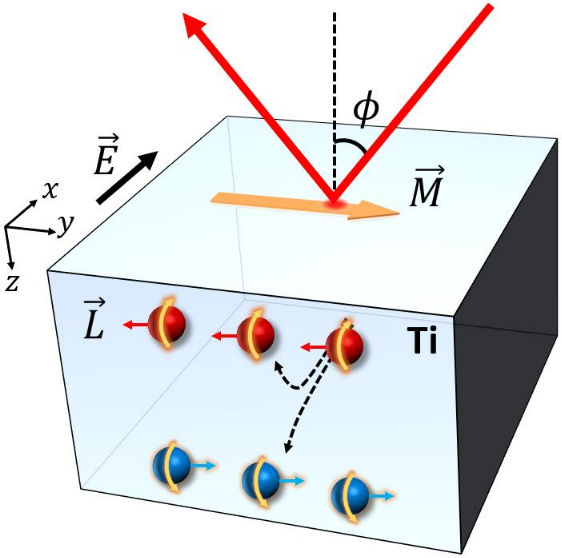

**Experiment**

Young-Gwan Choi at SKKU

**Theory**

Daegeun Jo at Postech

# Properties of Ti films

Crystal structure (XRD)

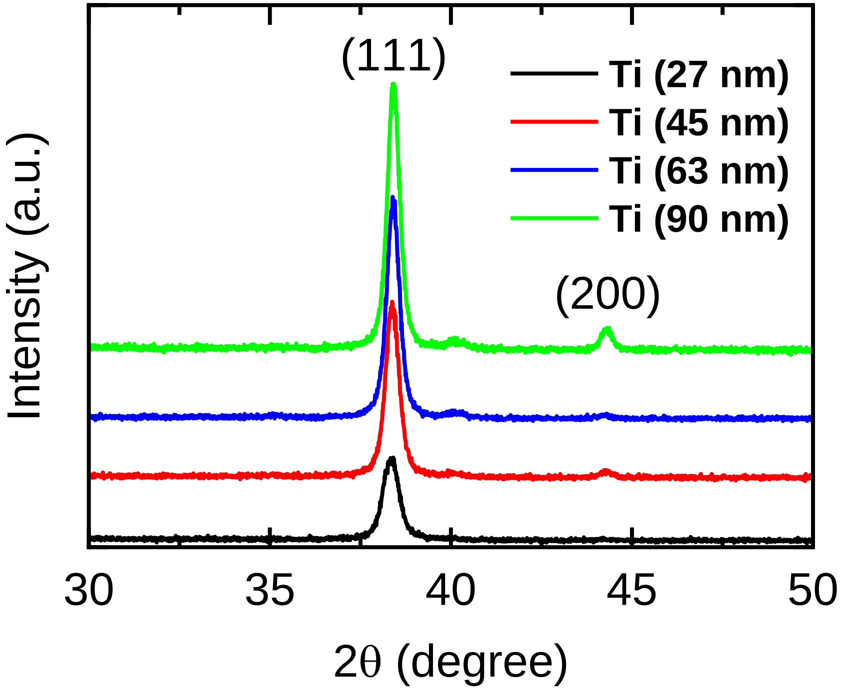

Electrical resistivity

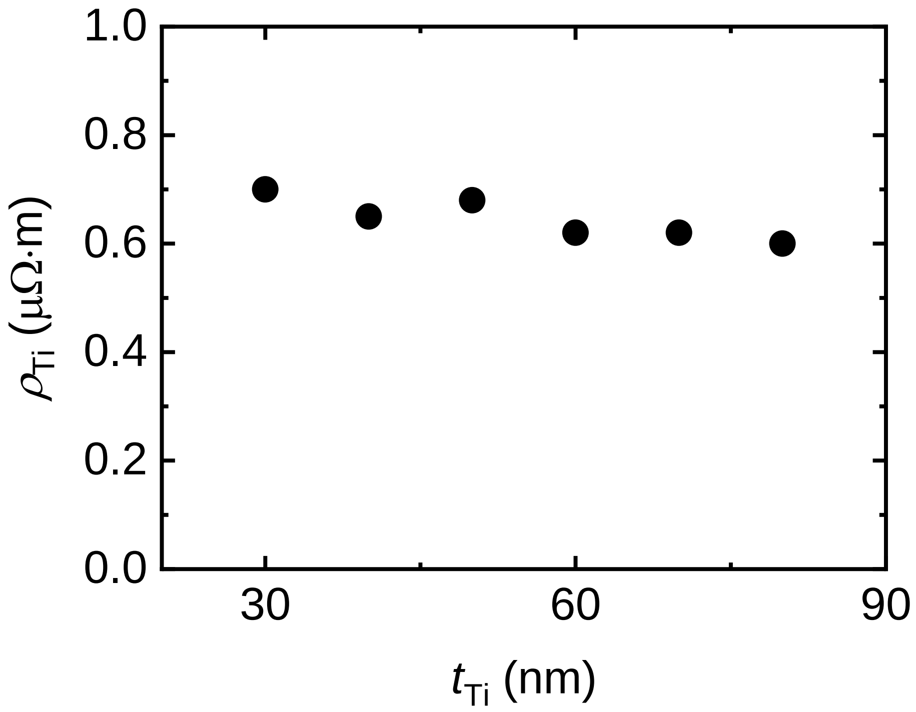

- ✓ Crystal structure: FCC structure with a dominant texture of (111)
- ✓ Resistivity: nearly thickness independent value of 0.6 μm·Ω.

# Current-induce MOKE in Ti

## Cross view

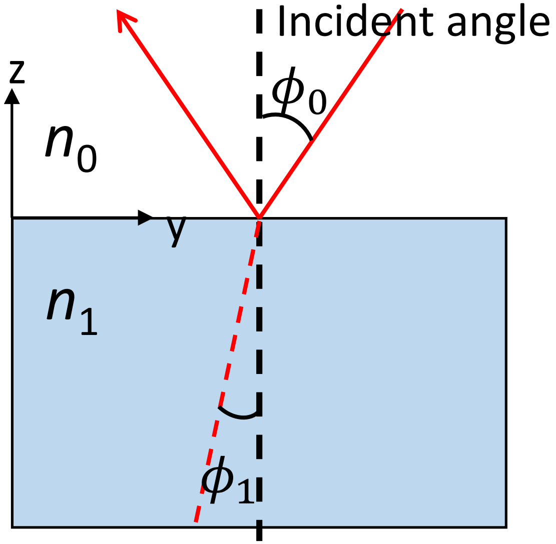

## Top view

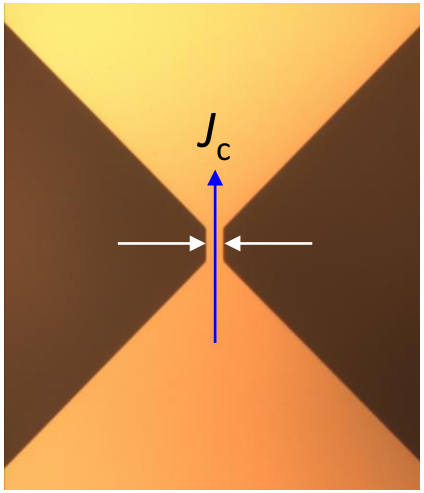

## MOKE with ± $\phi_0$

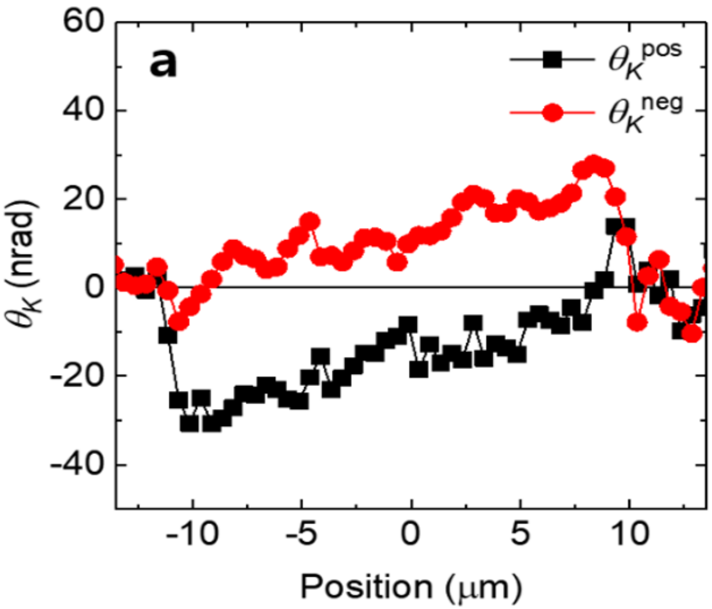

$$\theta_K^{tot} = \theta_K^P + \theta_K^L$$

Polar MOKE from $M_z$

Longitudinal MOKE from $M_y$

# Distinction between $M_z$ and $M_y$

**Channel position dependence**

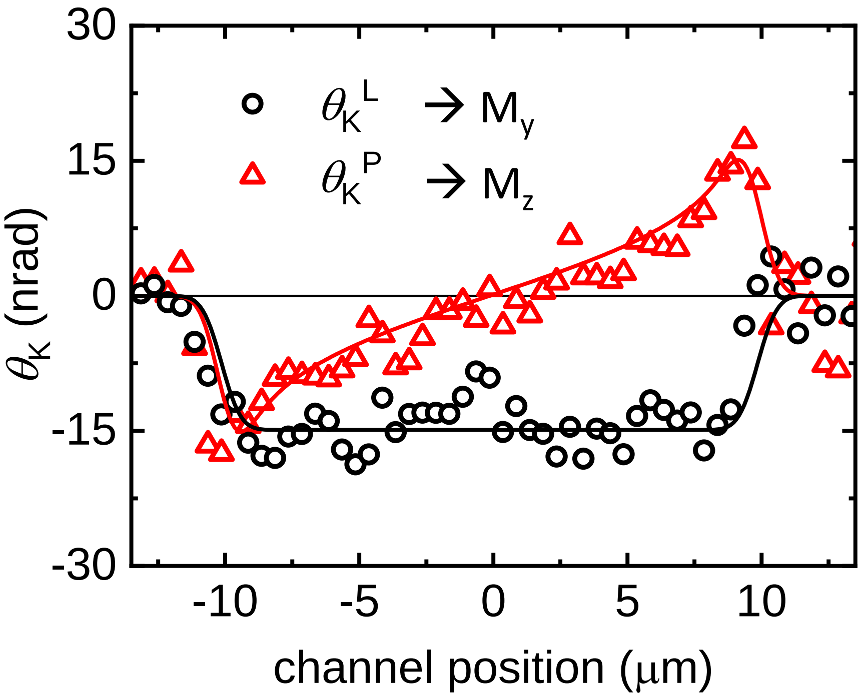

**Current density dependence**

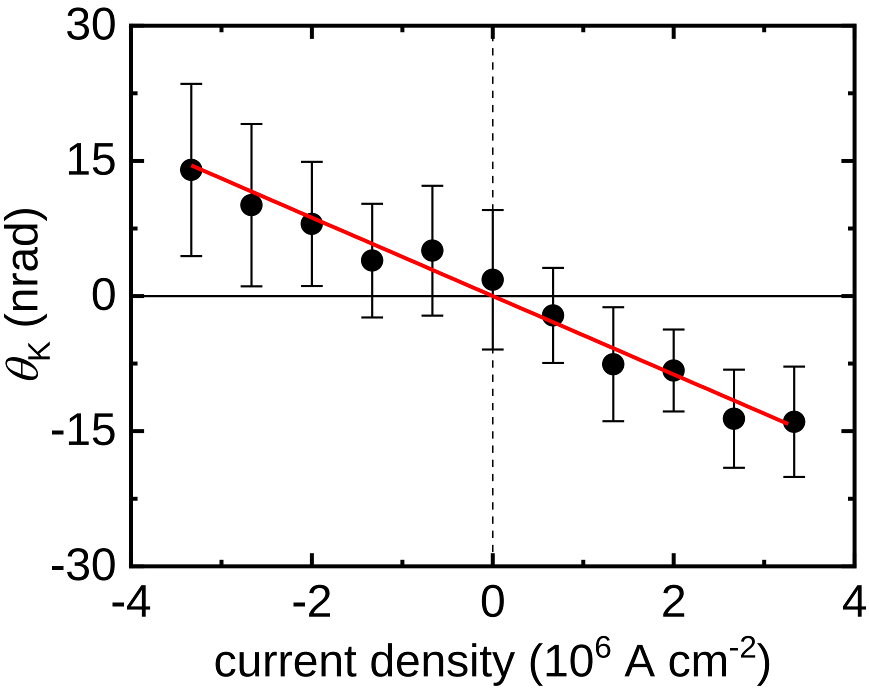

LMOKE: $$\theta_K^L = \frac{\cos\phi_0 \tan\phi_1}{\cos(\phi_0 - \phi_1)} \frac{i n_0 n_1 Q}{(n_1^2 - n_0^2)}$$

LMOKE changes its sign with the opposite incidence angle, whereas PMOKE does not.

# Reference sample for the Oersted field

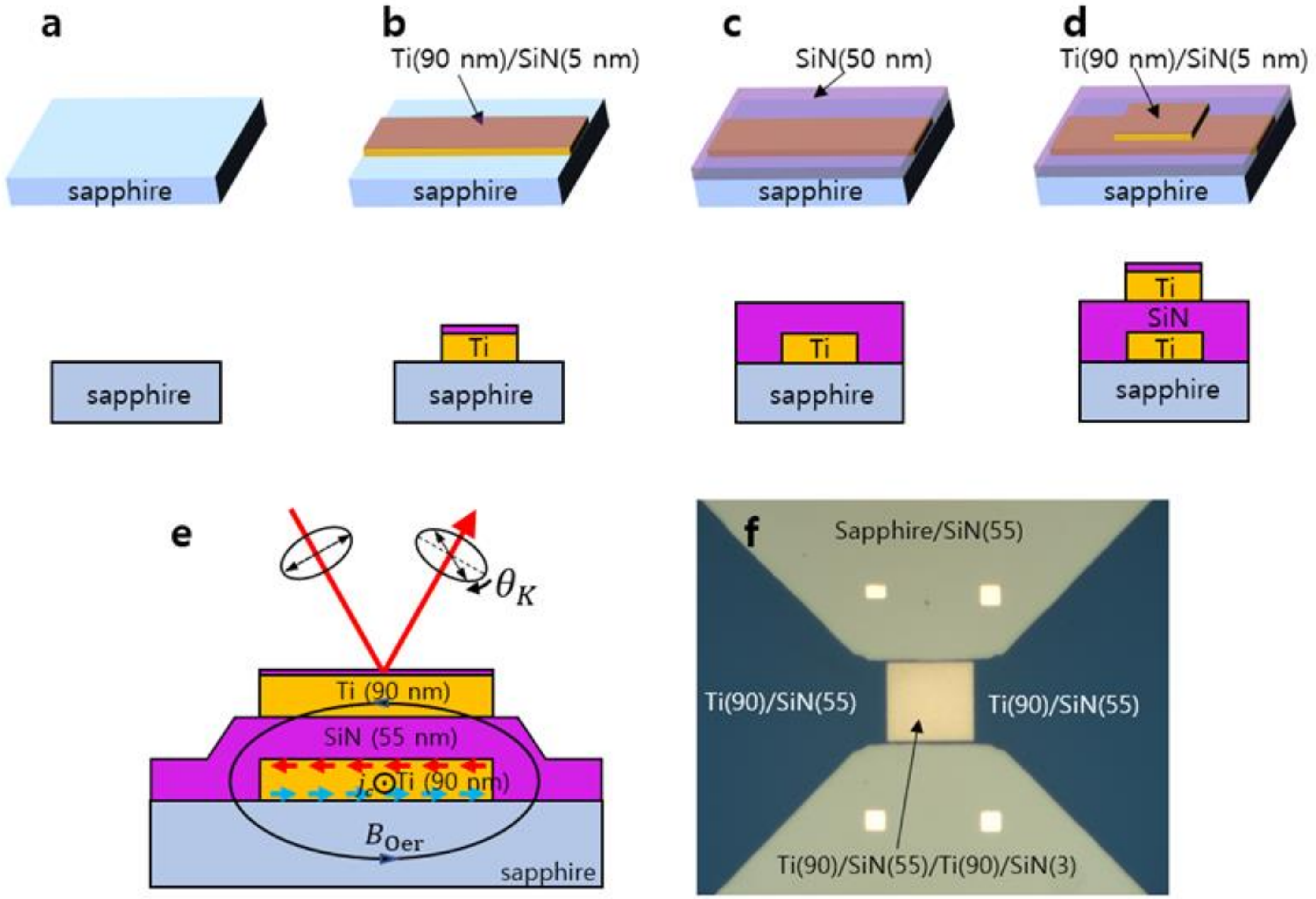

# Reference sample for the Oersted field

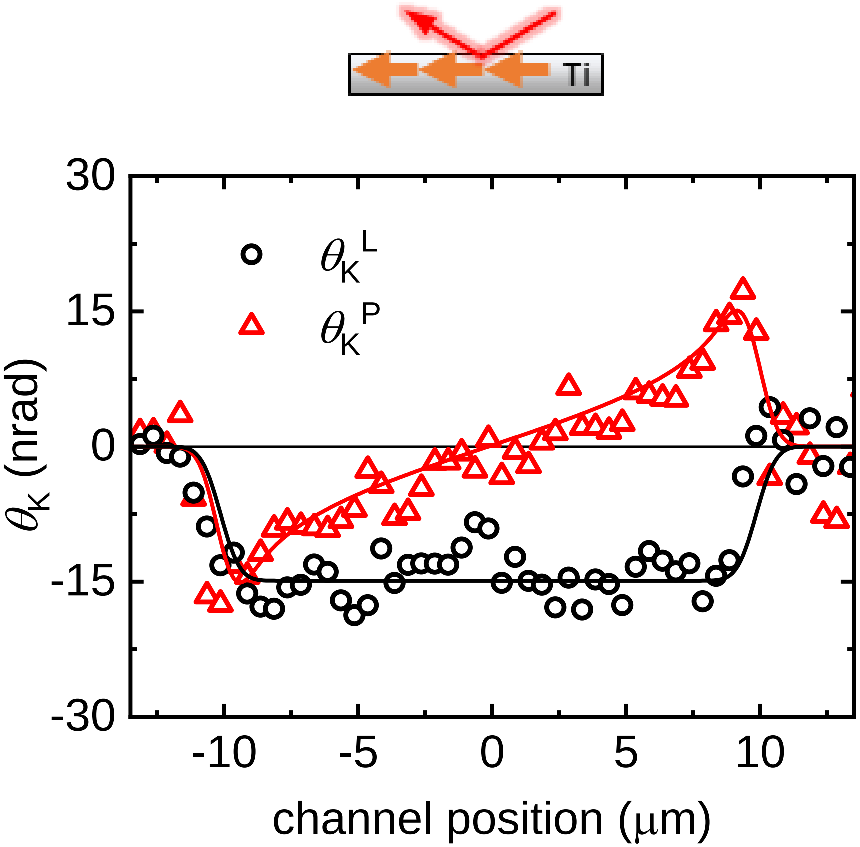

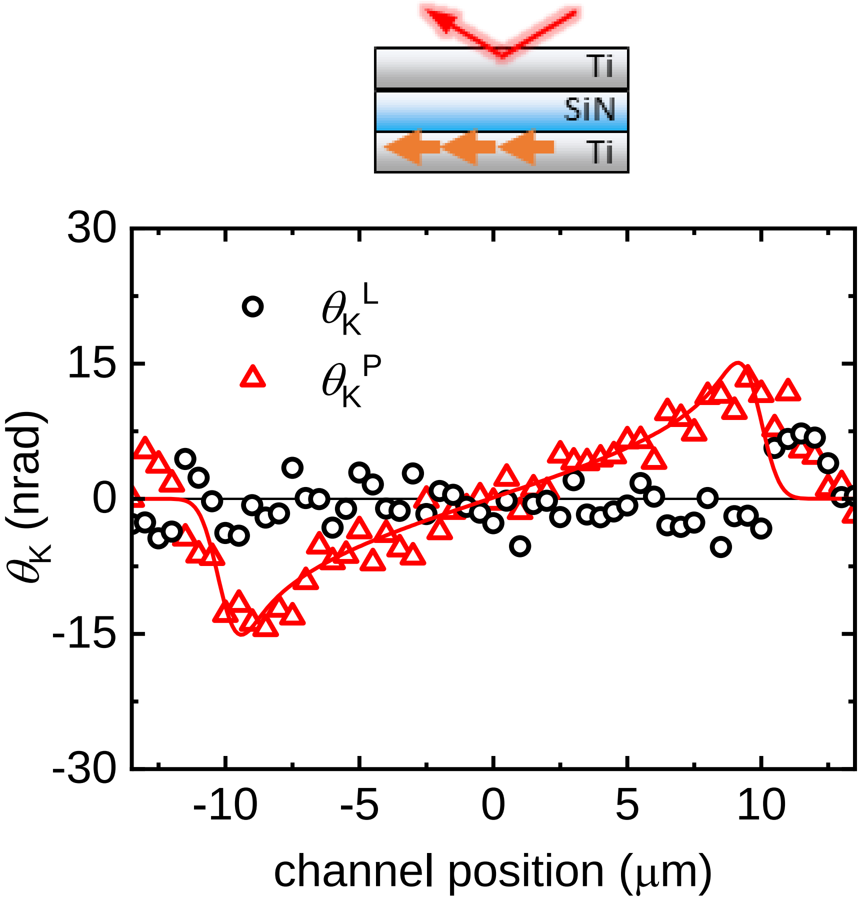

- ✓ PMOKE comes from the Oersted field.
- ✓ LMOKE does not come from the Oersted field.

# Estimation of the Oersted field

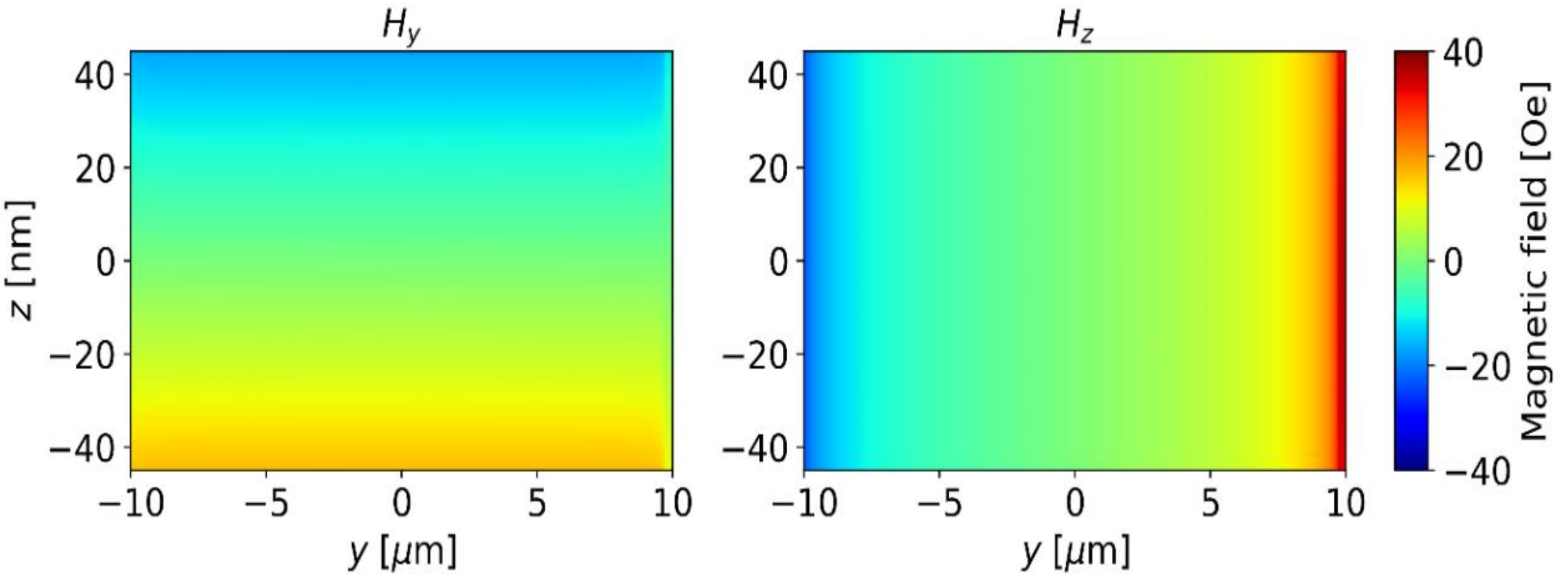

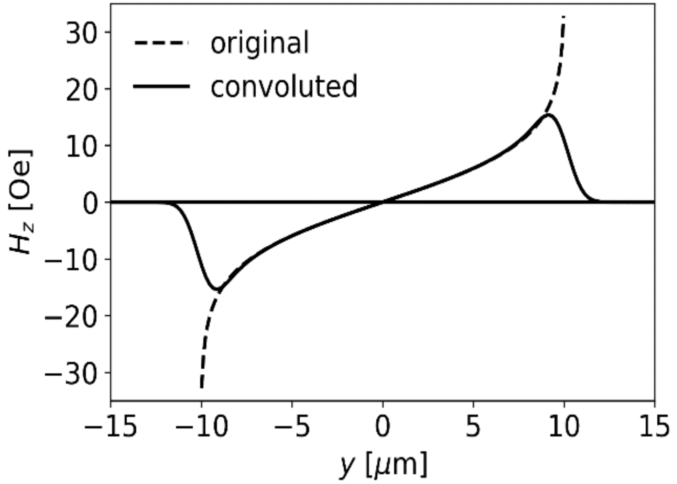

The spatial profile of $h_{\mathrm{Oe\_z}}$ matches to PMOKE.

At the channel edge,

$$h_{Oe\_z} = 15\ \mathrm{Oe} \Leftrightarrow \theta_K^P = 15\ \mathrm{nrad}$$

# Magneto-optic constant from $\theta_K^P$

$\Delta M = \chi H_{\text{ext}}$ , $\chi$ is magnetic susceptibility from orbital and spin.

Orbital contribution: van Vleck paramagnetism

$$\chi_{\text{orb}} = \frac{\mu_0 \mu_B^2}{N_{\boldsymbol{k}} \mathrm{V}_{\text{cell}} \hbar^2} \sum_{\boldsymbol{k}} \sum_{n,m} (f_{m\boldsymbol{k}} - f_{n\boldsymbol{k}}) \frac{\langle u_{n\boldsymbol{k}} | L_z | u_{m\boldsymbol{k}} \rangle \langle u_{m\boldsymbol{k}} | L_z | u_{n\boldsymbol{k}} \rangle}{E_{n\boldsymbol{k}} - E_{m\boldsymbol{k}} + i\Gamma} = 8.7 \times 10^{-6} \text{ emu/cc}$$

→ Consistent with a previous report: Grechnev, Low Temp. Phys. **35**, 638 (2009)

$Q^{\text{unit}} = -0.25 + i0.44 \left(\frac{\mu_{\text{B}}}{\text{atom}}\right)^{-1}$ for orbital magnetization

→ $Q^{\text{unit}}$ well explains the measured PMOKE by Oersted field.

→ $Q^{\text{unit}}$ is 100 times larger for orbital than spin.

# Ti thickness dependence of $\theta_K^L$

LMOKE of Ti as function of Ti thickness

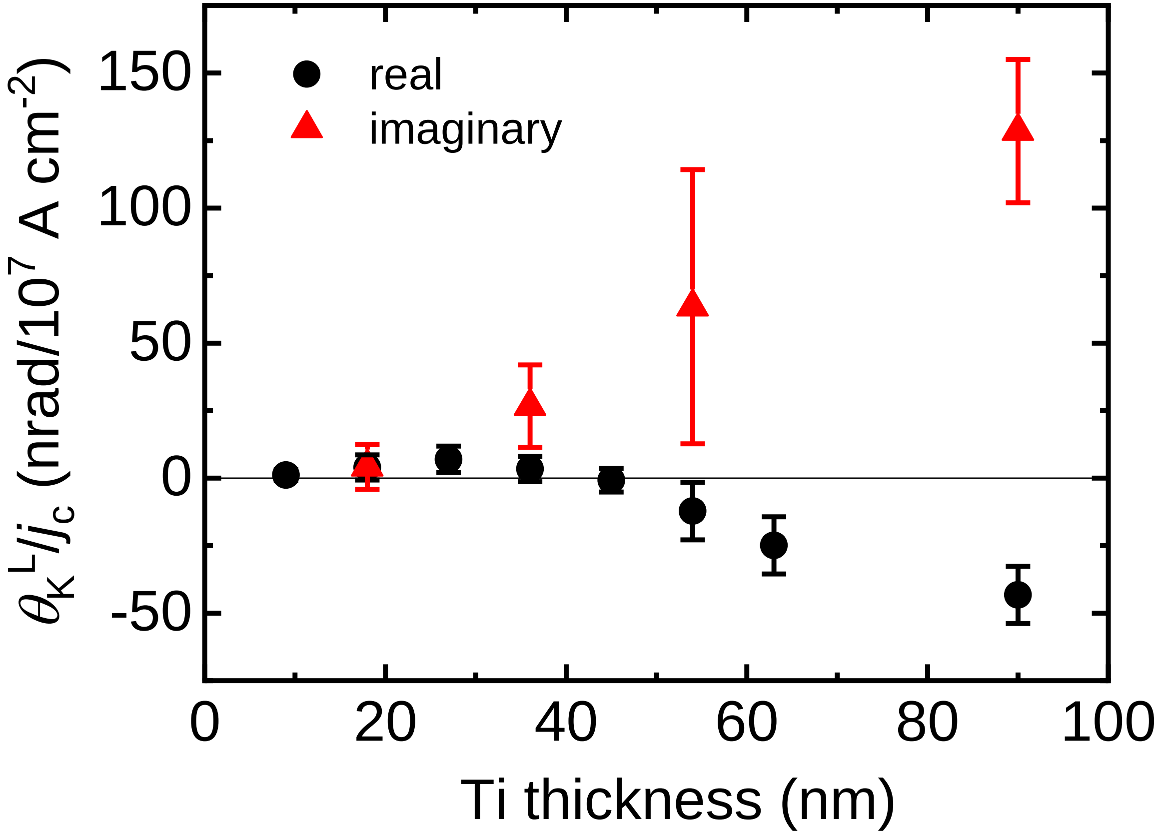

$$\tilde{\theta}_K^L = \underset{\substack{\uparrow \\ \text{real}}}{\theta_K^L} + \underset{\substack{\uparrow \\ \text{imaginary}}}{\varepsilon_K^L}$$

- ✓ Imaginary part is larger than real part.
- ✓ Real part changes its sign at $d_{Ti}$~45 nm.

# Comparison to Kerr rotation of Pt

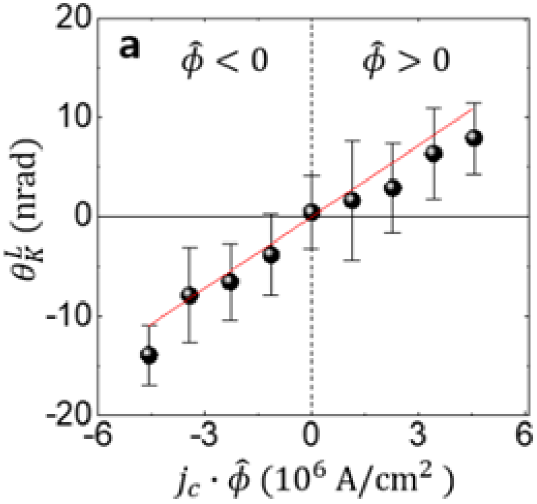

**Current dependence**

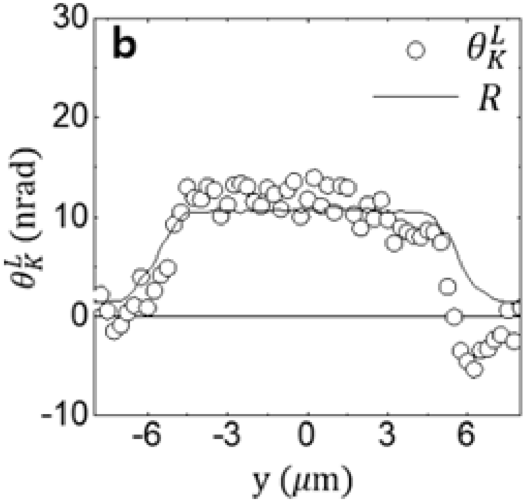

**Position dependence**

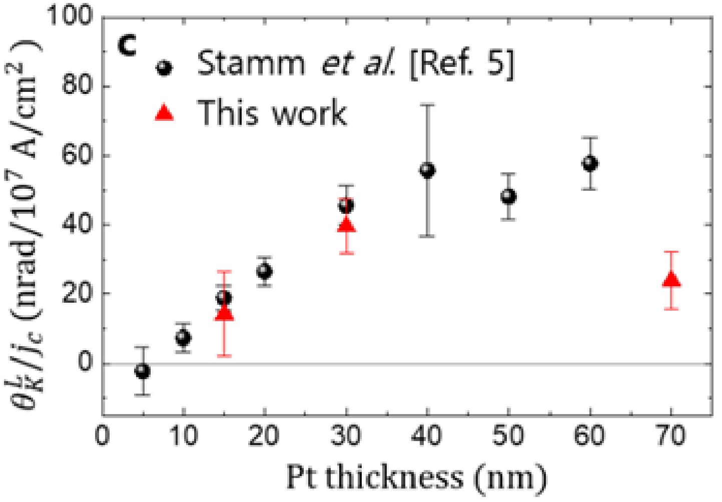

**Thickness dependence**

Reference: Stamm, PRL (2017)

- ✓ Magnitude of LMOKE on Pt is comparable to that on Ti.
- ✓ It is known that LMOKE on Pt is driven by SHE because of the strong SOC.
- ✓ LMOKE saturates at Pt thickness ~30 nm.

# Consideration of orbital profile

Kerr rotation from uniform magnetization ($\mu_B$ per atom)

$\alpha\ (t)$ : Effect of non-uniform distribution

$$\theta_K(t) = \theta_K^0 \overbrace{\int_0^t M_y(z) \cdot \kappa e^{\kappa z}}\,dz$$

orbital profile

Light penetration

$$\kappa = \frac{4\pi i n_1 \cos\theta_1}{\lambda}$$

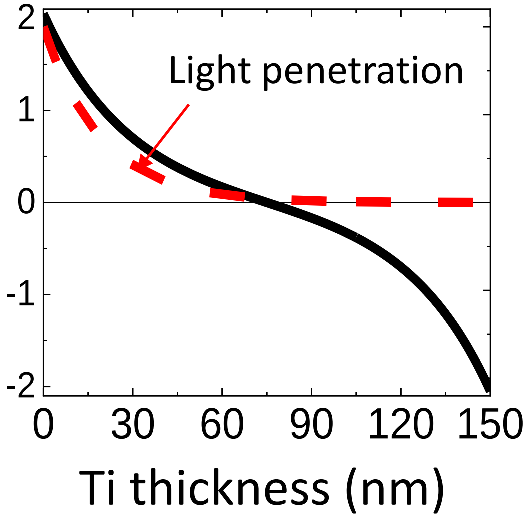

$$\theta_K^0 = \frac{\cos\phi_0 \tan\phi_1}{\cos(\phi_0-\phi_1)} \frac{i n_0 n_1 Q^{\mathrm{unit}}}{(n_1^2 - n_0^2)}$$

$$Q^{\mathrm{unit}} = -0.25 + i0.44 \left(\frac{\mu_\mathrm{B}}{\mathrm{atom}}\right)^{-1}$$

Theory: Tight-binding calculation

Experiment: Oersted field

# Orbital profile through thickness

Orbital continuity equation

$$\frac{\partial L_y}{\partial t} + \nabla \cdot \mathbf{J}^{L_y} = -\frac{L_y}{\tau_L}$$

$$J_i^{L_j} = -D_L \nabla_i L_j + \sigma_{\mathrm{OH}} \varepsilon_{ijk} E_k$$

At steady state,

$$\frac{\partial^2 L_y}{\partial z^2} = \frac{L_y}{l_L^2}, \text{where } l_L = (D_L \tau_L)^{1/2}$$

Boundary condition, $J_z^{L_y}(\mathrm{z}) = 0$ at the top (*z*=0) and the bottom (*z*=*t*) surfaces

$$M_y(t) = M_0 \frac{\sinh\left(\frac{t-2z}{2l_L}\right)}{\cosh\left(\frac{t}{2l_L}\right)}$$

$$M_0 = \gamma_L \sigma_{OH} \tau_L j_c \rho$$

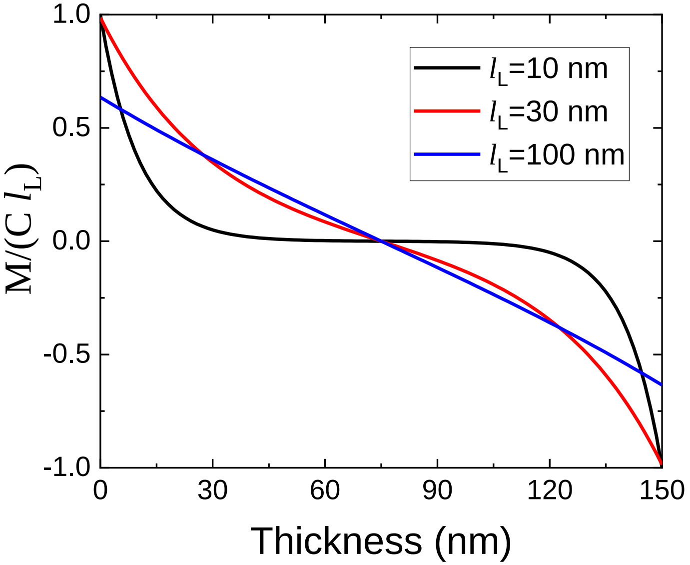

Orbital profile

# Effect of orbital diffusion length

$$\alpha\ (t) = \int_0^t M_y(z) \cdot \kappa e^{\kappa z}\, dz$$

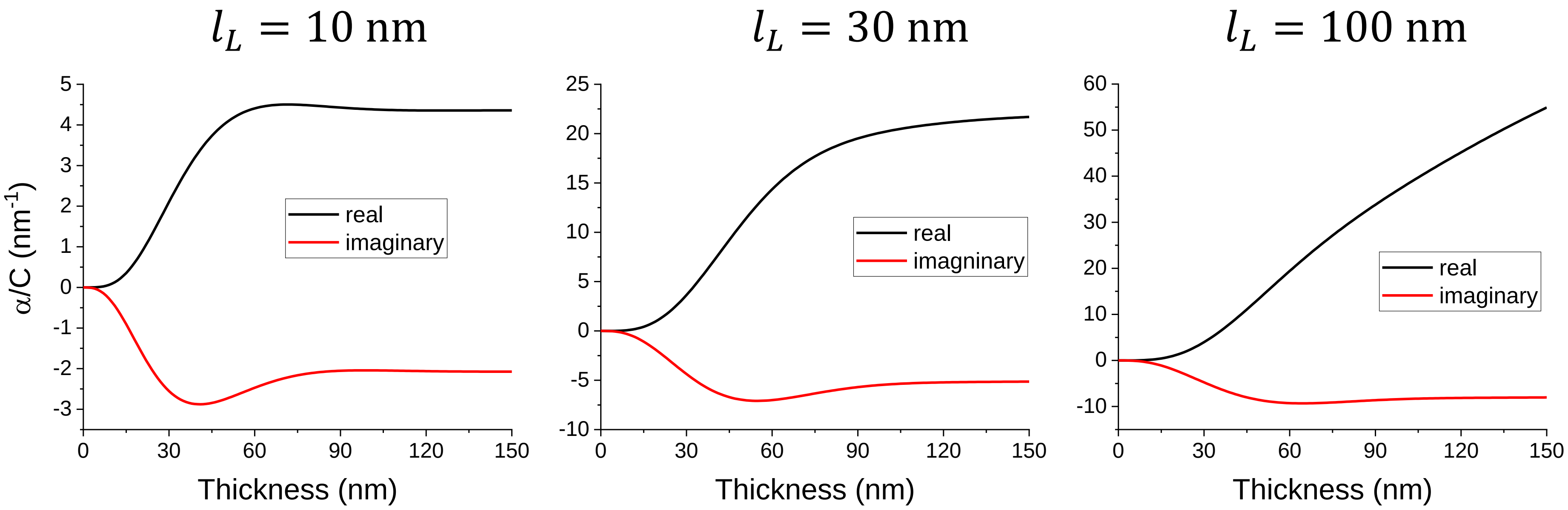

$l_L = 10\ \mathrm{nm}$ $l_L = 30\ \mathrm{nm}$ $l_L = 100\ \mathrm{nm}$

Orbital diffusion length → { Magnitude of orbital accumulation
Strong thickness dependence

# Determination of orbital diffusion length

Calculation: $\theta_K(t) = \theta_K^0 \alpha(t)$

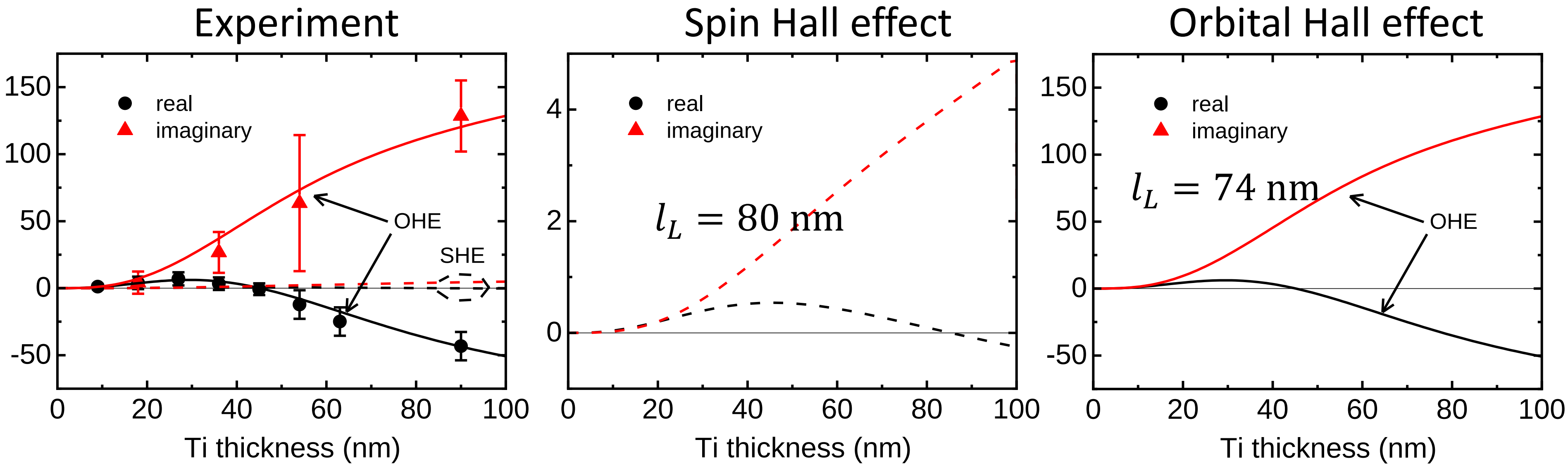

$$\sigma_{\mathrm{SH}} = -40\ (\hbar/e)(\Omega \cdot \mathrm{cm})^{-1} \qquad R \times \sigma_{\mathrm{OH}} = +40\ (\hbar/e)(\Omega \cdot \mathrm{cm})^{-1}$$

$$Q^{\mathrm{unit}} = 0.002 - i0.006 \qquad Q^{\mathrm{unit}} = -0.25 + i0.44$$

Thickness dependence of MOKE is explained by $l_L$ of 74 nm.

Magnitude of MOKE is explained by $R \times \sigma_{\mathrm{OH}}$.

↑

orbital quenching by crystal field

# Magnitude of MOKE: SHE vs OHE

## Kerr rotation from spin Hall effect

Spin Hall conductivity

$$\sigma_{\mathrm{SH}} = -40\ (\hbar/e)(\Omega\cdot\mathrm{cm})^{-1}$$

Magneto-optic constant for spin

$$Q_{\mathrm{spin}}^{\mathrm{unit}} = 0.002 - i0.006$$

$\theta_K^L$ of ~1 nrad, too small

## Kerr rotation from orbital Hall effect

Orbital Hall conductivity

$$\sigma_{\mathrm{OH}} = +3800\ (\hbar/e)(\Omega\cdot\mathrm{cm})^{-1}$$

+orbital quenching

$$R \times \sigma_{\mathrm{OH}} = +40\ (\hbar/e)(\Omega\cdot\mathrm{cm})^{-1}$$

Magneto-optic constant for orbital

$$Q_{\mathrm{spin}}^{\mathrm{unit}} = -0.25 + i0.44$$

→ Confirmed by the Oersted-field-induced $\theta_K^P$

$\theta_K^L$ of ~100 nrad

# Part 2: orbital torque

## Orbital torque

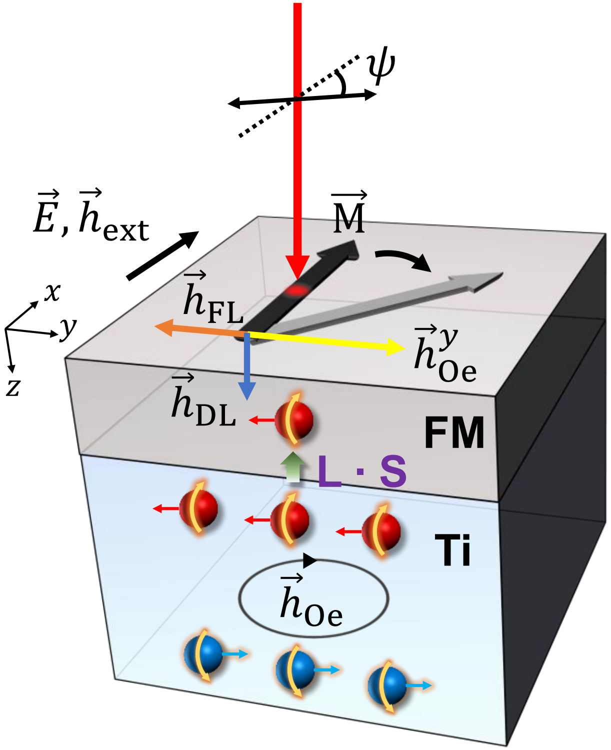

**Experiment**

Kyung-Hun Ko at SKKU

**Theory**

Daegeun Jo at Postech

# Sample structure for torque measurement

Ti/FM bilayer

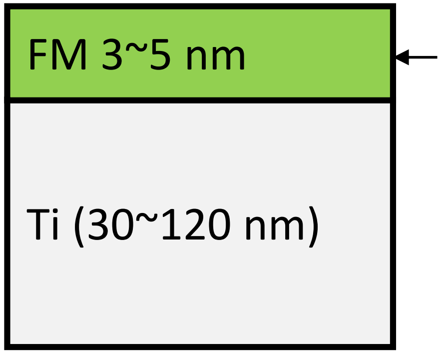
FM 3~5 nm

Ti (30~120 nm)

Ni, Co, CoFeB

Ti/Pt/FM bilayer

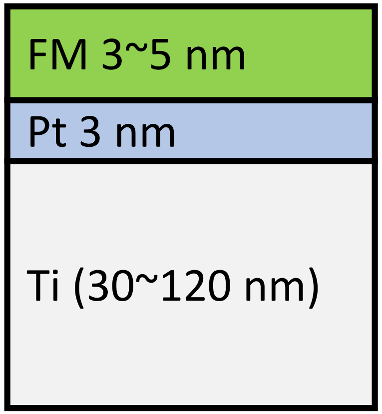
FM 3~5 nm

Pt 3 nm

Ti (30~120 nm)

# Magnetic properties of FM

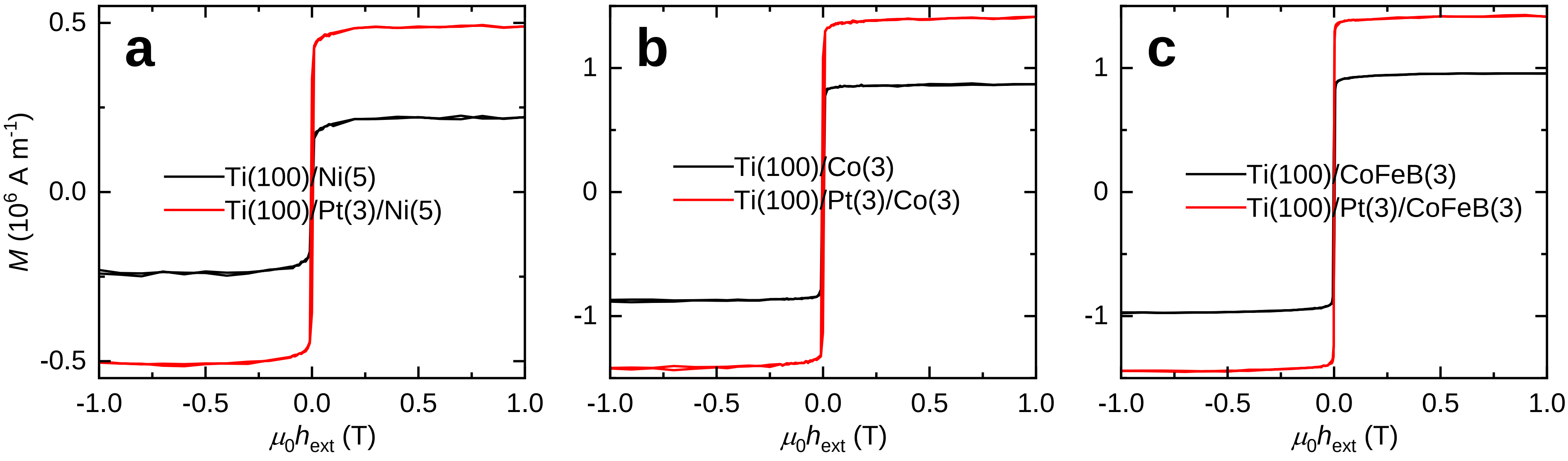

Ti/Ni, Ti/Pt/Ni

Ti/Co, Ti/Pt/Co

Ti/CoFeB, Ti/Pt/CoFeB

- ✓ Significant reduction of magnetization in Ti/FM structure.
- ✓ Magnetization of FM recovers its bulk value with Pt insertion.

# Intermixing effect on magnetization

Ni-Ti phase diagram

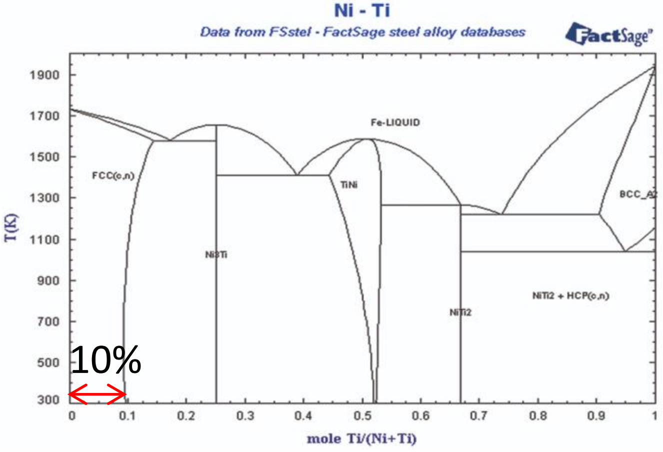

Ni-Pt phase diagram

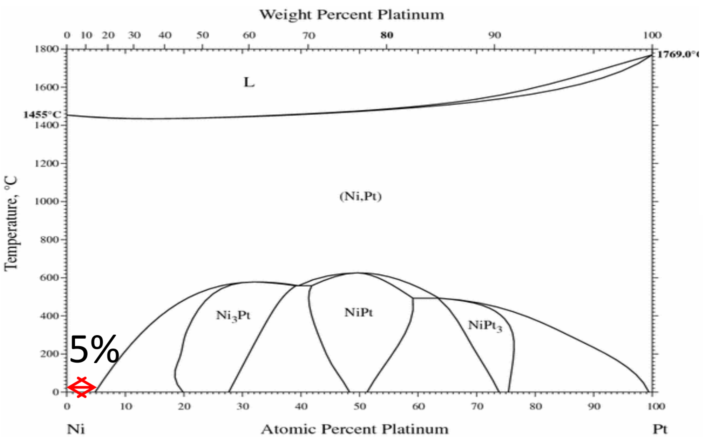

Doping effect on exchange stiffness of permalloy

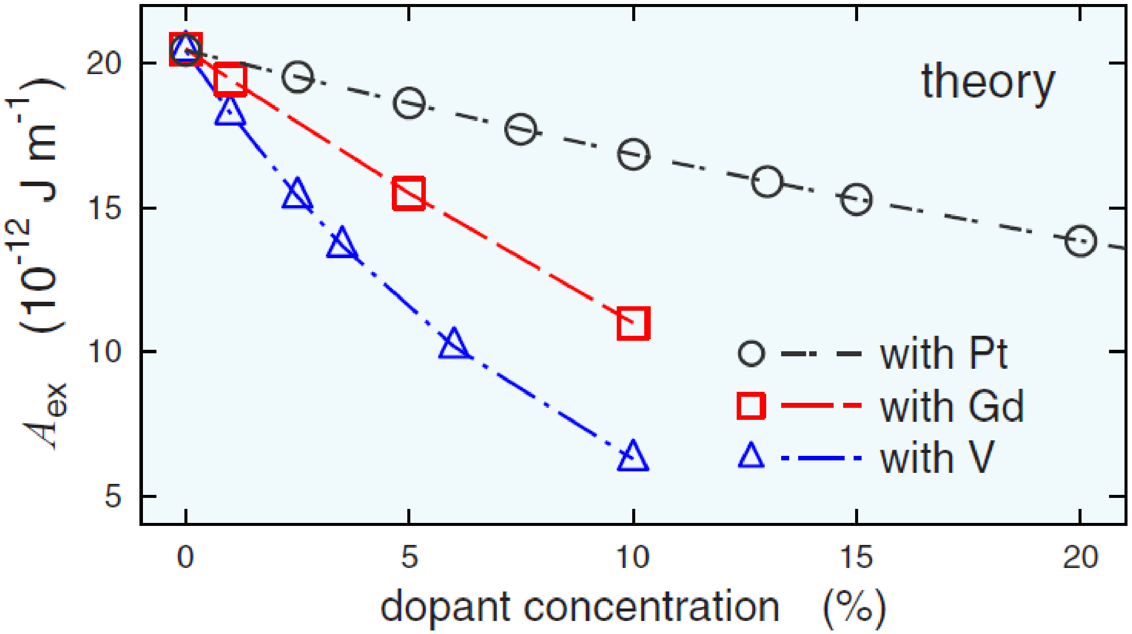

PRB 100, 024435 (2019)

Some element degrades ferromagnetic order quickly.

# Kerr rotation from ferromagnet

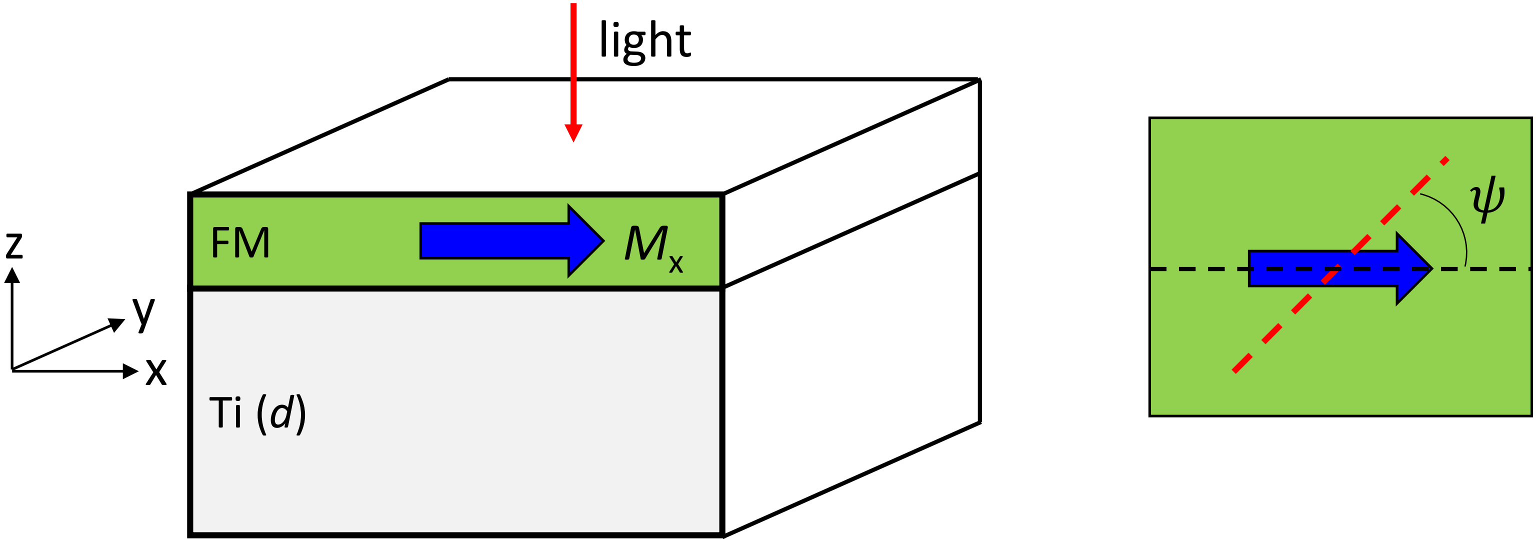

quadratic magneto-optic coefficient

Linear magneto-optic coefficient

Light polarization angle

$$\Delta\theta_K = \alpha_{\mathrm{MO}}\Delta M_z + \beta_{\mathrm{MO}}\cos 2\psi\,\Delta M_y$$

$h_{\mathrm{DL}} + h_{\mathrm{Oe}}^{\mathrm{z}}$

$h_{\mathrm{FL}} + h_{\mathrm{Oe}}^{\mathrm{y}}$

Damping-like torque

Field-like torque

z-part of Oersted field

y-part of Oersted field

# Light polarization angle dependence

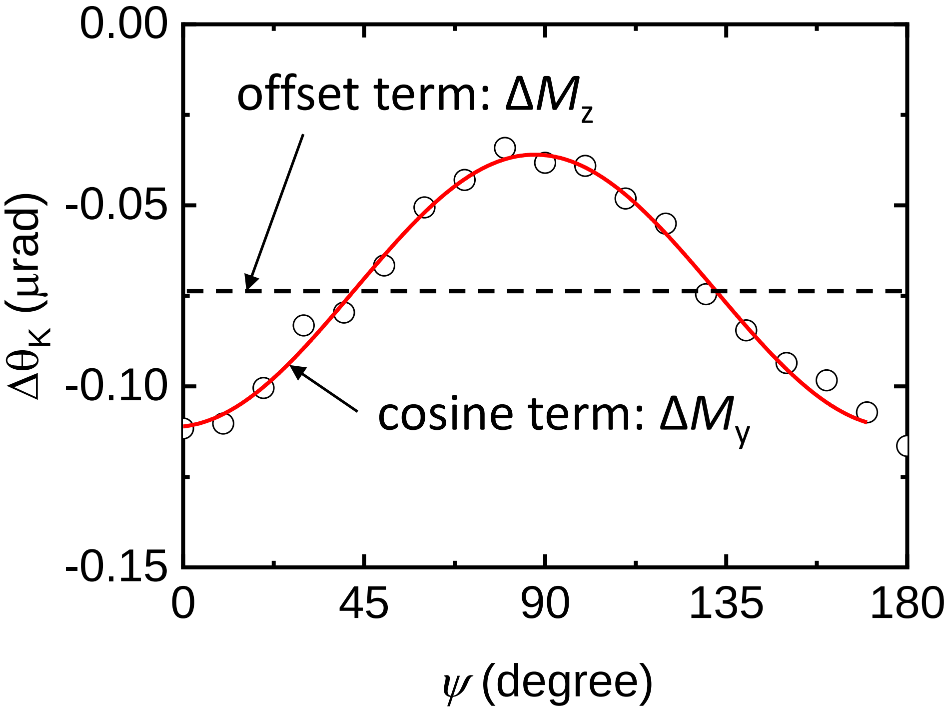

Ti (100 nm)/Ni (5 nm)

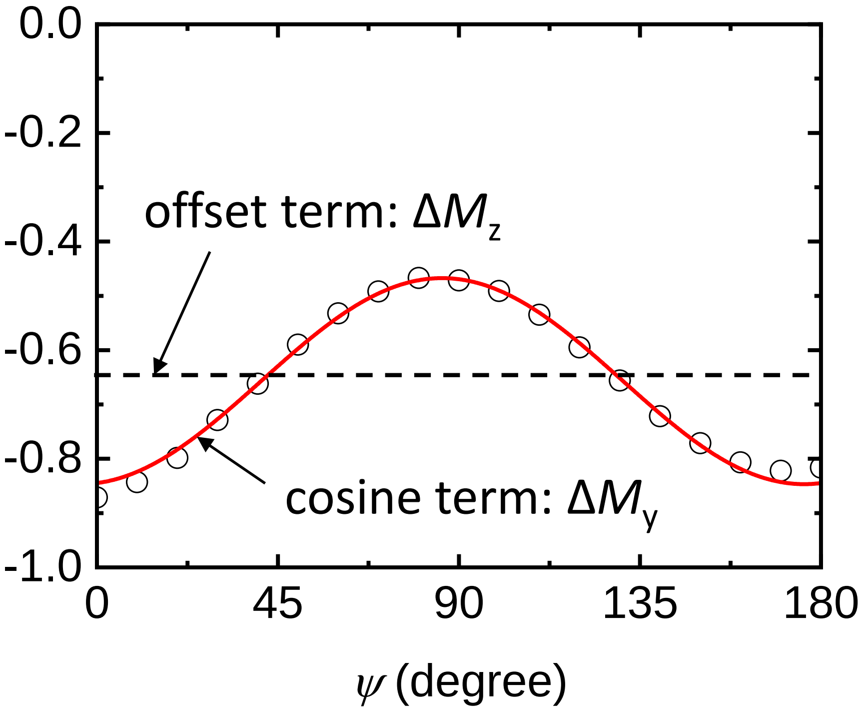

Ti (100 nm)/Pt (3 nm)/Ni (5 nm)

✓ $M_z$ and $M_y$ can be distinguished from the polarization angle dependence.

# External field dependence

$$\Delta M_z = \frac{h_{\mathrm{DL}} + h_{\mathrm{Oe}}^{\mathrm{z}}}{h_{\mathrm{ext}} + M_{\mathrm{eff}}} \approx \frac{h_{\mathrm{DL}} + h_{\mathrm{Oe}}^{\mathrm{z}}}{M_{\mathrm{eff}}},$$

→ nearly independent on $h_{\mathrm{ext}}$

$$\Delta M_y = \frac{h_{\mathrm{FL}} + h_{\mathrm{Oe}}^{\mathrm{y}}}{h_{\mathrm{ext}} + h_{\mathrm{ani}}} \approx \frac{h_{\mathrm{FL}} + h_{\mathrm{Oe}}^{\mathrm{y}}}{h_{\mathrm{ext}}}$$

→ $1/h_{\mathrm{ext}}$ dependence

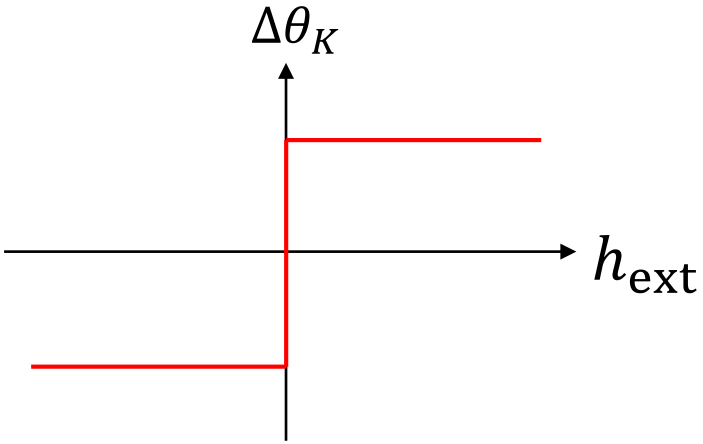

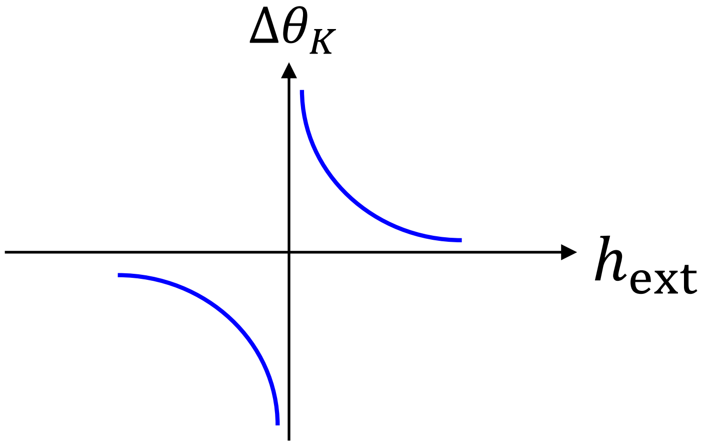

✓ $M_z$ and $M_y$ can be distinguished from the magnetic field dependence.

# External field dependence

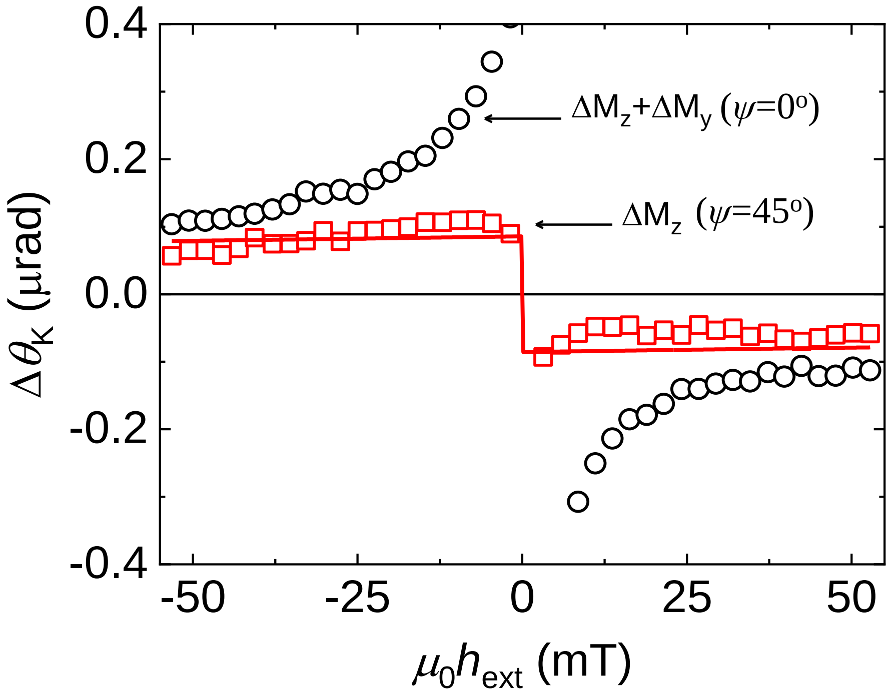
Ti (100 nm)/Ni (5 nm)

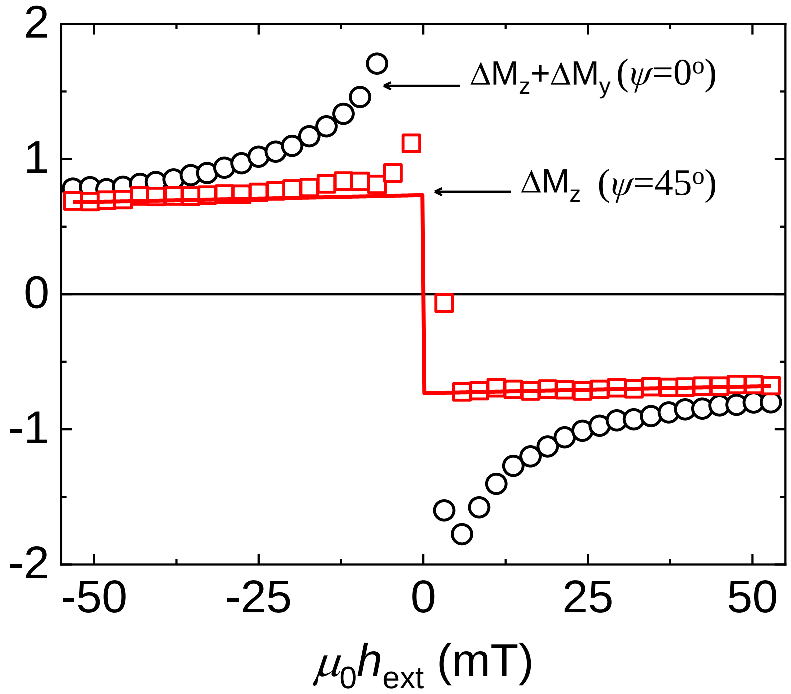
Ti (100 nm)/Pt (3 nm)/Ni (5 nm)

- ✓ $\Delta M_z$-driven $\Delta\theta_K$: $\Delta\theta_K$ ($\psi$=45°)
- ✓ $\Delta M_y$-driven $\Delta\theta_K$: $\Delta\theta_K$ ($\psi$=0°) − $\Delta\theta_K$ ($\psi$=45°)

# DLT analysis: ΔM$_z$ of Ti/Pt/Ni

Scanning along channel position (y)

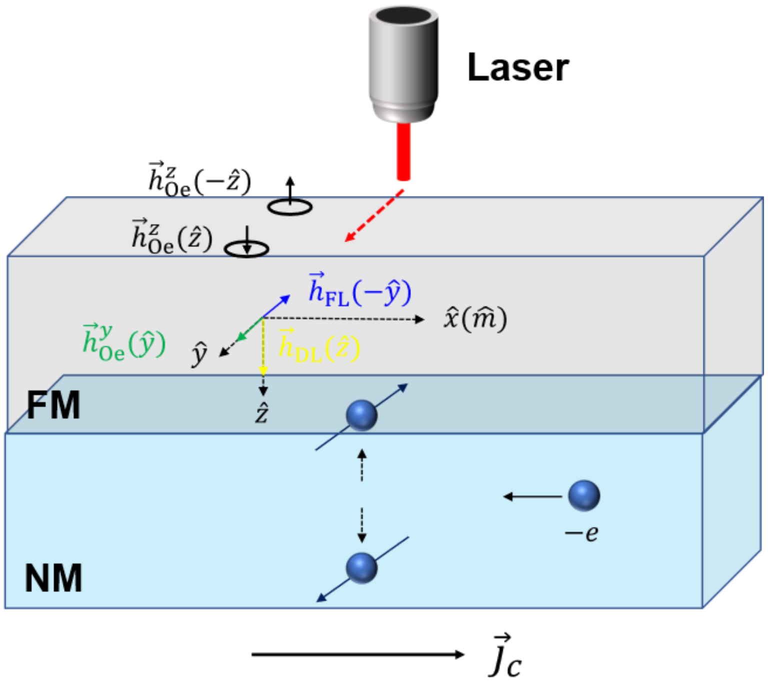

Ti (100 nm)/Pt (3 nm)/Ni (5 nm)

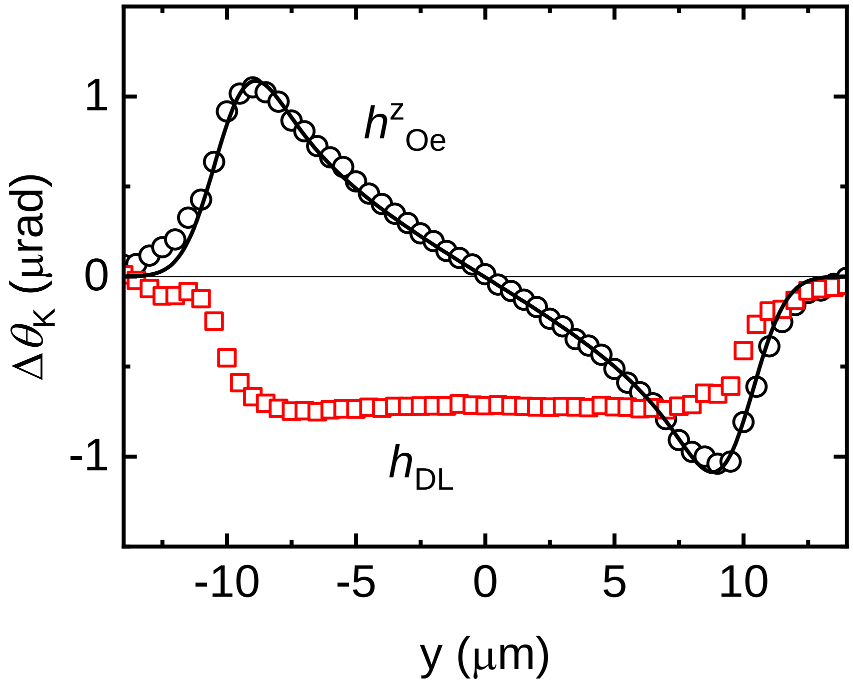

$$\Delta M_z \approx \frac{h_{\mathrm{DL}} + h^z_{\mathrm{Oe}}}{M_{\mathrm{eff}}} \begin{cases} h^z_{\mathrm{Oe}}(y) = \frac{I}{2\pi w}\ln\frac{y}{w-y}, \text{ antisymmetric on y} \\ h_{\mathrm{DL}}, \text{ independent on y} \end{cases}$$

# Ti thickness dependence of DLT

**Torque efficiency vs Ti thickness**

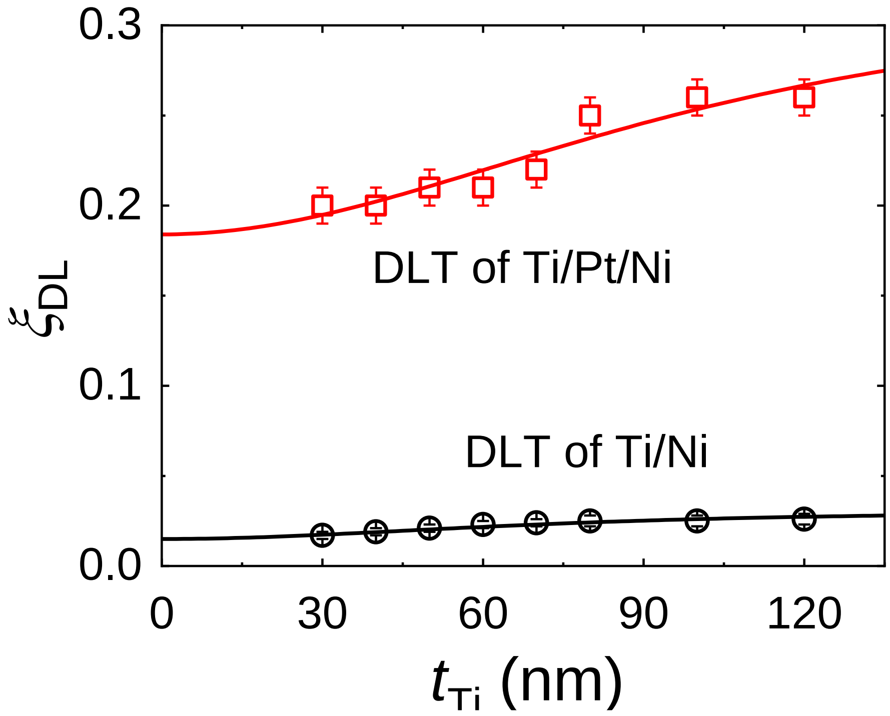

$$\xi_{DL} = \frac{2e}{\hbar} M_s t_{FM} \frac{h_{DL}}{j_c}$$

$$\xi_{DL} = \theta_{OH}^{eff}\left(1 - \mathrm{sech}\left(\frac{t_{Ti}}{l_L}\right)\right) + \xi_0$$

$$\xi_0 = \theta_{SH}^{Pt} \times \frac{j_{Pt}}{j_{Ti}}$$

Ti/Ni

$$\begin{cases} l_L = 50 \pm 15\ \mathrm{nm} \\ \theta_{OH}^{eff} = 0.015 \pm 0.003 \\ \xi_0 = 0.015 \pm 0.002 \end{cases}$$

Ti/Pt/Ni

$$\begin{cases} l_L = 70 \pm 20\ \mathrm{nm} \\ \theta_{OH}^{eff} = 0.13 \pm 0.01 \\ \xi_0 = 0.18 \pm 0.015 \end{cases}$$

# FLT analysis: $\Delta M_y$

AC charge-current-driven $\Delta M_y$

AC magnetic-field-driven $\Delta M_y$

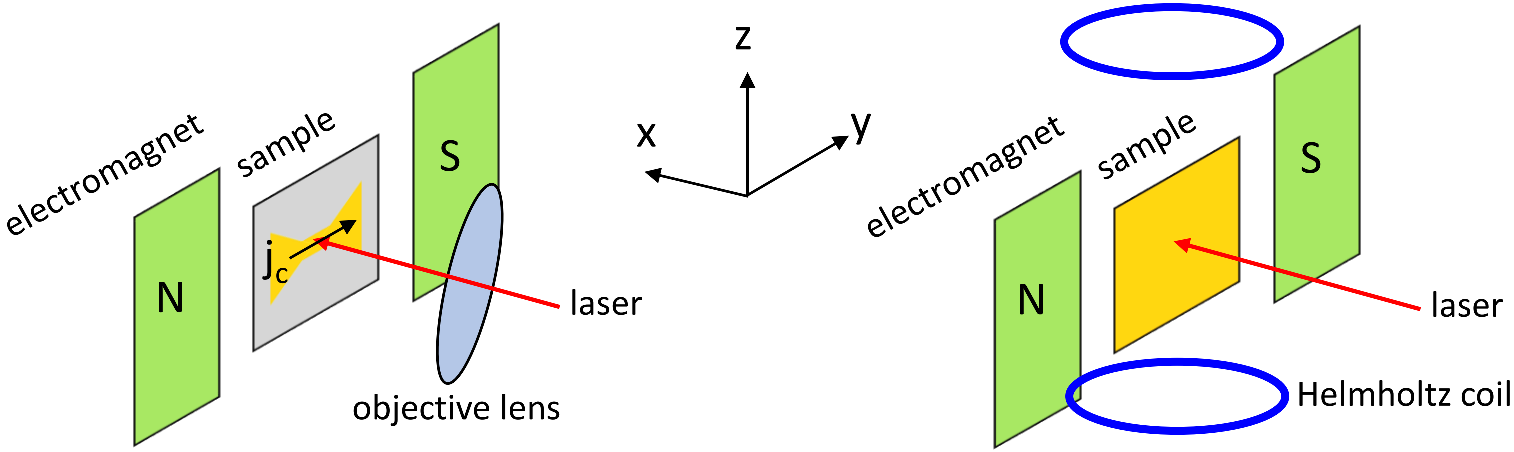

$h_{\mathrm{DL}} + h_{\mathrm{Oe}}^{\mathrm{y}}$

$h_{\mathrm{Helmholtz}}^{\mathrm{y}}$

# FLT analysis: $\Delta M_y$ of Ti/Co

## sub/Ti (100 nm)/Co (3 nm)

AC charge-current-driven $\Delta M_y$ | AC magnetic-field-driven $\Delta M_y$

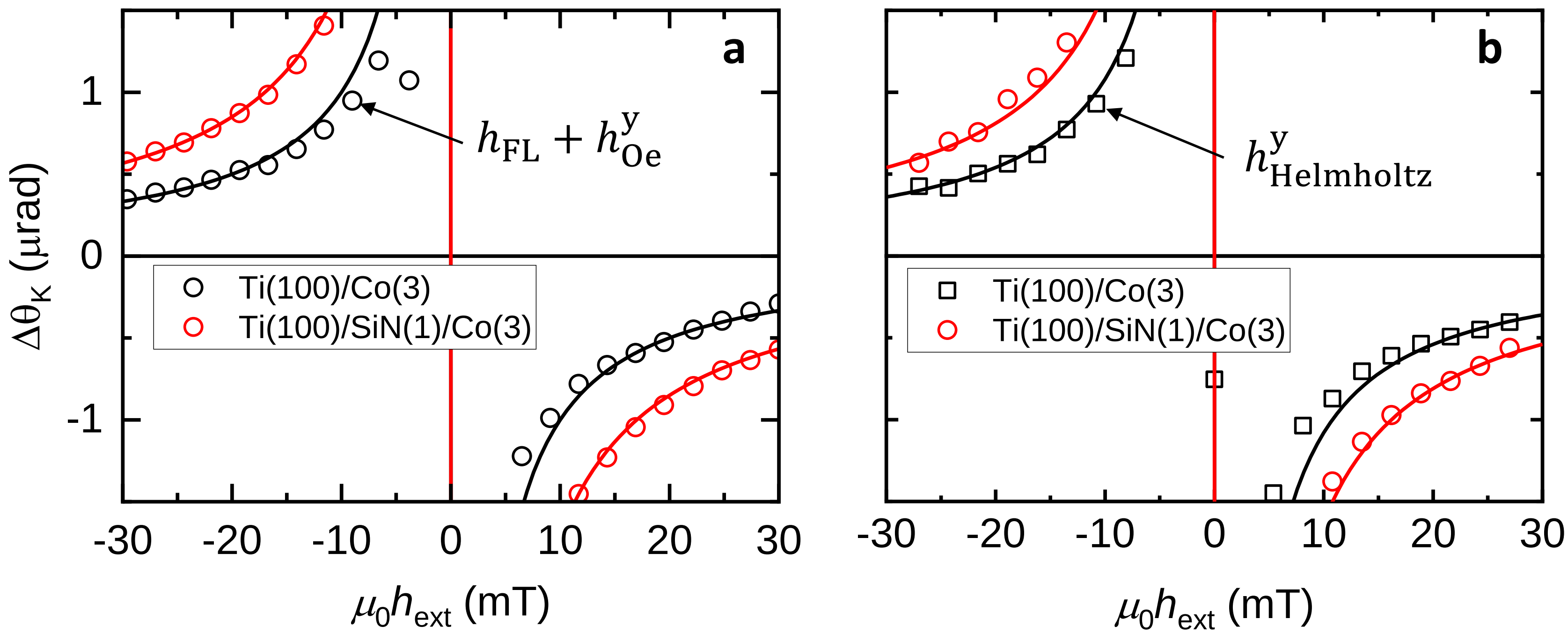

$$\Delta\theta_K^{\text{quadratic}} = \beta_{MO}\Delta M_y$$

- ✓ $\beta_{MO}$ is sensitive on the film structure
- ✓ Weak FLT in Ti/Co structure.

# FLT analysis: $\Delta M_y$ of Ti/Pt/Ni

## sub/Ti (100 nm)/Pt (3 nm)/Ni (5 nm)

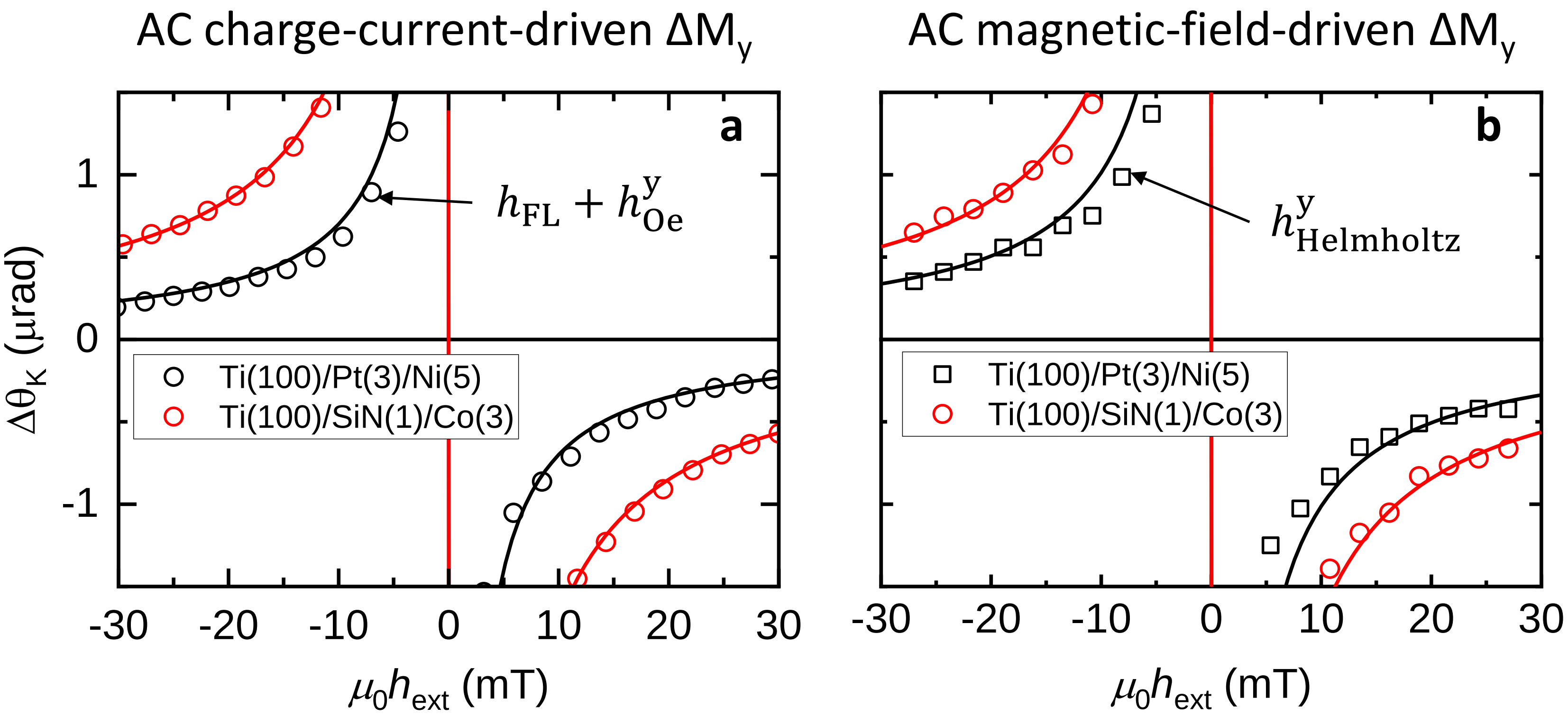

AC charge-current-driven $\Delta M_y$

AC magnetic-field-driven $\Delta M_y$

- ✓ Significant FLT in Ti/Pt/Ni structure.

# Ti thickness dependence of FLT

Torque efficiency vs Ti thickness

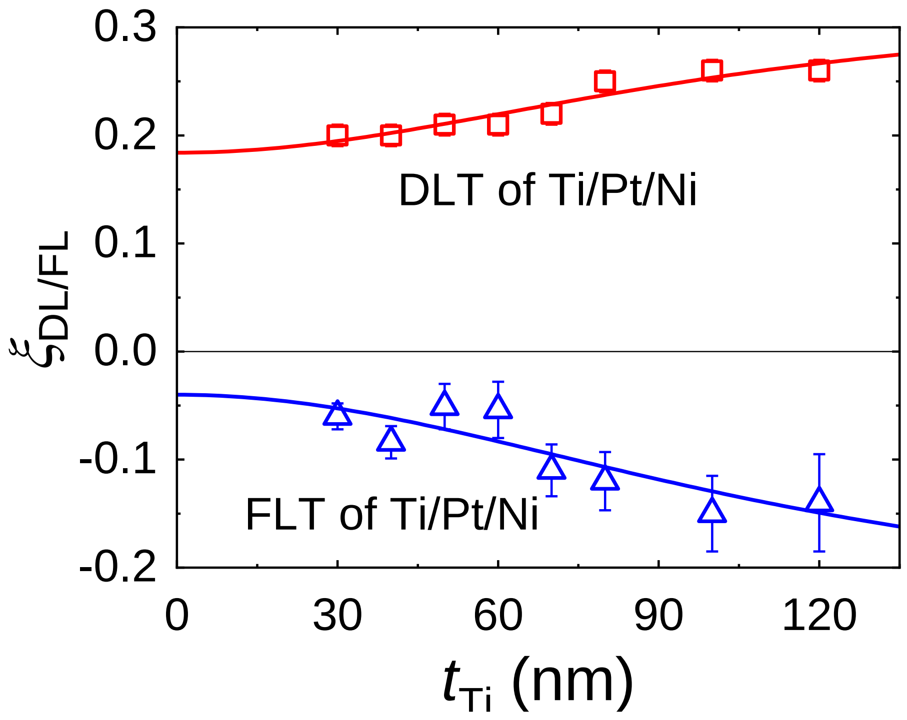

DLT

$$l_L = 70 \pm 20 \text{ nm}$$

$$\theta_{\mathrm{OH}}^{\mathrm{eff}} = 0.13 \pm 0.01$$

$$\xi_0 = 0.18 \pm 0.015$$

FLT

$$l_L = 80 \pm 30 \text{ nm}$$

$$\theta_{\mathrm{OH}}^{\mathrm{eff}} = -0.19 \pm 0.05$$

$$\xi_0 = -0.04 \pm 0.02$$

- ✓ $l_L$ of 70~80 nm is consistent with orbital accumulation result.
- ✓ DLT and FLT are comparable in magnitude.

# Summary

## Orbital accumulation

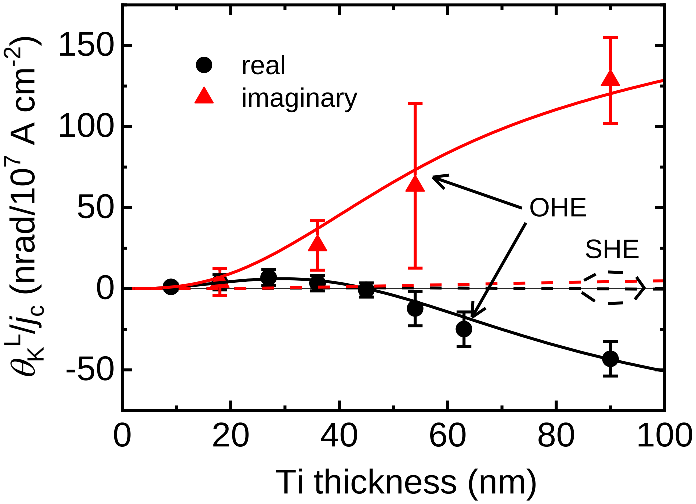

Strong LMOKE on Ti, comparable to that on Pt

→ cannot be explained with SHE

Ti thickness dependence

→ $l_L$ of 74 nm

LMOKE magnitude

→ $R \times \sigma_{\mathrm{OH}} = +40\ (\hbar/e)(\Omega \cdot \mathrm{cm})^{-1}$

## Orbital torque

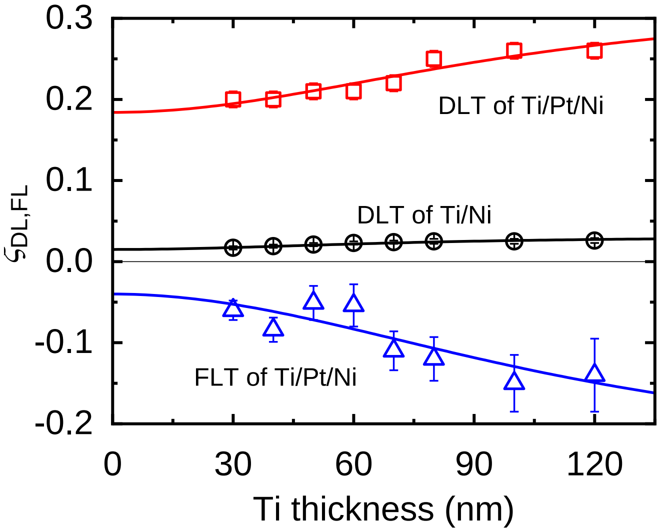

Significant DLT and FLT from Ti

→ cannot be explained with spin torque

Ti thickness dependence.

→ $l_L$ of 70~80 nm.

DLT magnitude

→ $\theta_{\mathrm{OH}}$ of 0.13 ($\sigma_{\mathrm{OH}}$ of 1100 $(\hbar/e)(\Omega \cdot \mathrm{cm})^{-1}$